1968

An investigation of filler effects in a silicone resin molding compound

Robert Owen Bridges
Lehigh University

AN INVESTIGATION OF FILLER EFFECTS IN A SILICONE RESIN MOLDING COMPOUND

by

Robert Owen Bridges

A Thesis

Presented to the Graduate Committee

of Lehigh University

in Candidacy for the Degree of

Master of Science

in Metallurgy and Materials Science

Lehigh University

1968

CERTIFICATE OF APPROVAL

This thesis is accepted and approved in partial fulfillment of the requirements for the degree of Master of Science.

May 17, 1968
Date

John D. Hanson
Professor in Charge

Chairman of the Department of
Metallurgy and Materials Science

ACKNOWLEDGEMENTS

The author wishes to express sincere appreciation to Dr. J. A. Manson for his guidance during the course of this investigation and for his suggestions in the preparation of the text. Sincere appreciation is expressed to Mr. G. J. Kookootsedes of the Dow Corning Co. for supplying the material used in this investigation and for his advice on experimental procedures. Thanks also go to Dr. D. I. Marshall of the Engineering Research Center for his advice and counsel.

The author also wishes to express his appreciation to Dr. L. S. Sperling and Tony Galanti of Lehigh University for performing flexural tests, to Mr. L. L. Lynch for performing thermal expansion measurements, and to others too numerous to mention. Last, but by no means least, my thanks go to the Western Electric Company for sponsoring the graduate studies of which this thesis is a part.

TABLE OF CONTENTS

TABLE OF CONTENTS (cont'd)

LIST OF FIGURES

LIST OF FIGURES (cont.)

LIST OF TABLES

ABSTRACT

The effects of the silica filler concentration and distribution of filler particle sizes on selected mechanical, thermal, electrical and rheological properties of a silicone resin molding compound have been investigated. In addition, the rheological properties have been investigated as a function of temperature and shear rate for one filler concentration. Tensile strength, modulus, toughness, and dielectric constant increase with filler concentration. At the same time there is a decrease in ultimate elongation, thermal expansion and mold shrinkage. The mechanical properties are substantially unaffected by changes in the filler particle size distribution within the range of this experiment (~ 9 to 24 μ). The minimum apparent viscosity is not a strong function of filler concentration below concentrations of 63% (by volume); beyond this point the viscosity increases rapidly. The viscosity at fixed filler concentration decreases substantially with temperature at a constant shear rate, and with shear rate at a constant temperature.

I - INTRODUCTION

This investigation was undertaken in order to determine the effect of filler concentration and filler particle size on the mechanical and physical properties of a silicone molding compound with the objective of finding the resin filler combination which has the best balance of properties. The flow properties were also investigated as a function of temperature and shear rate. Information gained from these tests is useful in determining optimum molding conditions.

Silicone resin molding compounds are being used extensively in the electronics industry as an encapsulating material for electronic components. Their wide acceptance is, to a great extent, due to the following factors:

(1) They will not contaminate the sensitive electronic components.

(2) They will withstand temperatures in excess of 250°C for extended periods of time.

(3) They are economically favorable when compared with other methods of encapsulation.

The chief disadvantage of this material as it is presently formulated is its extreme brittleness as indicated by the relatively high modulus and low strength. This brittleness can lead to failure by cracking during thermal shock because the thermal expansion of the silicone is on the order of two to three times that of the metals which are normally used as connecting leads and supports

for electronic devices. A more compatable material would result if it were possible to increase the strength while decreasing the modulus and thermal expansion.

In view of the vast effect which filler concentration and filler particle size have on the properties of other polymer-filler systems, it seems reasonable to look to these filler characteristics as a means of improving the overall properties of the material. However, any change in formulation must be considered in view of its effect on flow properties for it is these properties which determine the ease with which the material can be molded.

A - Resin vs. Rubber

Silicone resins are one class of a rather large group of materials known as silicones. The structural diagram for a typical resin which illustrates the curing reaction is shown in Figure 1. This material is characterized by the silicon-oxygen-silicon chain which is common to all silicones[1].

Silicone resins are the hardest and most rigid of the silicones[1]. Their structure differs from that of the more familiar silicone rubber in that they are cross-linked at many more points. This increased cross-link density constrains the motion of the molecules and, as a result, the internal motion on deformation is due largely to stretching of the chemical bonds rather than by uncoiling of the molecules as is the case with rubber[1]. Considerable literature is available on the effect of fillers on the properties of polymers in general which includes a number of articles on silicone rubber,

but little or no information on filled silicone resins is available. However, a study of the literature gives some insight in the filler-polymer interaction which is helpful in understanding the silicone resin-filler system.

B - Effect of Fillers

The viscosity of a solvent containing a small volume concentration of rigid spheres in suspension follows the Einstein viscosity law, [2]

$$\eta^* = \eta \left[1 + 2.5\ V_f\right] \qquad (1)$$

where η^* and η are the viscosity of the emulsion and solvent respectively, and V_f is the volume concentration of the filler. Guth, [2] by extending this theory to Young's Modulus, showed the same basic relationship was followed provided additional terms were added to the equation,

$$E = E_o \left[1 + B_1 V_f + B_2 V_f^2 + B_3 V_f^3 \bullet\bullet\bullet\bullet\right] \qquad (2)$$

where E and E_o are the modulus of the solvent and emulsion and V_f is the filler volume concentration. B_1, B_2, B_3 ... are constant for spherical particles but must be modified somewhat for non-sperical fillers.

Guth [2] determined the coefficients for the rubber-carbon black system and found values of $B_1 = 2.5$, $B_2 = 14.1$. Using these values for the coefficients and neglecting the higher order terms, he found that experimental results agreed fairly well with theory up to volume concentrations of about 10%. While his treatment makes

allowances for particle shape, no consideration is given to the effect of particle size.

Cohan [3] investigated the effect of filler particle size in the rubber carbon-black system for particle diameters in the 10 to 40 mμ range. He found that the modulus was substantially independent of particle diameter. He also investigated the properties of natural rubber with calcium carbonate fillers and found that the modulus, as a function of filler concentration, agreed fairly well with the modulus predicted by Guth's equation up to 40% filler concentrations.

The effect of silica fillers on silicone rubbers is very pronounced. A. M. Bueche [4] has shown that the modulus of silica reinforced silicone rubbers increases much more rapidly than predicted by Guth's equation. The mechanism which leads to the improved properties is not clearly understood. It is generally agreed that the polymer is attached to the filler [4,5]. Whether the attachment is chemical or mechanical has not been clearly demonstrated. F. Bueche[6] attributes the increase in modulus over and above that predicted by equation (2) to strong bonding between polymer and filler surfaces which serves to increase the effective cross-link density.

The effect of fillers has been theoretically treated in terms of adhesion between polymer and filler by Sato and Furukawa[7] and in a somewhat more simple manner by Neilsen[8]. Both these treatments predict an increase in modulus and strength and a decrease in ultimate elongation as the filler concentration is increased. By

use of these theories the theoretical range of a property can be calculated by first assuming no adhesion and then perfect adhesion. Sato's treatment takes the filler size into account in a rather indirect manner; Neilson assumes that strength, modulus and elongation are independent of filler size.

Rehner[9] treated filler reinforcement from a thermodynamic point of view. He defines a "reinforcement energy", R.E., which occurs during isothermal mixing of an agregate of filler particles with the rubber. When the filler particle size is held constant, the change in energy on mixing is given by,

$$R.E. = a\left[(1 + V_f/V_r)^{2/3} - 1\right] - bV_f \qquad (3)$$

where a and b are constants and V_f and V_r are the volume fractions of filler and rubber respectively. When filler concentration is held constant the energy change during mixing as a function of filler particle size is given by

$$R.E. = a' - b'/d \qquad (4)$$

where a' and b' are constants and d is the filler particle diameter.

Rehner's theory predicts a decrease in R.E. as the filler concentration is increased and as the filler particle size is decreased. It is reasonable to assume that this lowering of energy results in the enhancement of material properties, but this is difficult to experimentally verify because the exact relationships between R.E. and properties such as modulus, tensile strength and thermal expansion which are normally measured are not known.

Alter [10] examined existing data from the literature in an effort to determine the relationship between filler particle size and material properties. He found that for constant filler concentrations the relative modulus of mineral filled polyethylene is given by

$$E/E_o = 1 + C/d \qquad (5)$$

where C is a constant. He also found linear relationships between 1/d and ultimate elongation and tensile strength.

Warrick and Lanterbur [11] reported a very pronounced increase in the tensile strength of Siloxane rubber as filler particle size was decreased. Their experiments were performed with silica filler particle diameters in the 5 to 150 mμ range.

No information on the effect of fillers on the properties of silicone resin compounds is available in the literature. However, because of their similarity to other polymer-filler systems, it is reasonable to expect relationships, similar to those found in other systems, to exist between the filler characteristics and the properties of the silicone resin compound.

C - Rheology

Silicone resin, in common with other thermosetting compounds, becomes a hard mass within a short time when molded under conditions of temperature and pressure. A number of tests to determine the flow and cure characteristics of thermosetting molding compounds have been devised. Perhaps the most useful are those which allow

the measurement of the force required to shear the material as a function of time at a constant temperature. Two methods for doing this which yield essentially the same data are described in the literature. In one method a torque rheometer is used [12] and in the other a capillary extrusion rheometer [13]. The extrusion rheometer, when set at a constant rate, yields a plot similar to that shown in Figure 2. From this plot the minimum shear stress, which is related to the minimum viscosity, and the time required for the material to harden can be determined. These parameters, which can be determined as a function of temperature and shear rate, are useful in determining the optimum molding temperature, pressure, and cure time.

The rheometer profile is also useful in evaluation of the effects of various material preparations. For example, the effect of filler concentration and particle size on minimum viscosity and flow time can be determined by this method.

II - EXPERIMENTAL PROCEDURE

A - Material

The material chosen for investigation is a silicone resin with a fused silica filler. It was supplied by the Dow Corning Company and consists of three material groupings. Group #1 is their comercially available QM-9-1090 compound with 75% by weight filler. Group #2 consists of seven lots of M-9-1090 material with the same filler particle size distribution as the Group #1 material but with filler concentrations ranging from 10 to 80% by weight. Group #3 consists of three lots of material with the same filler concentration as Group #1 but with filler particle size distributions which were obtained by fractionation of the standard filler into lots rated fine, medium, and coarse.

B - Properties Investigated

The properties which are the object of this investigation can be classified as either mechanical, thermal, electrical, or rheological.

1 - Mechanical Properties

a - Tensile Properties

An Instron universal testing machine was used to determine tensile properties. The results of a typical tensile test are shown in Figure 3. The force, which is related to the tensile stress, σ, by

$$\sigma = F/A \tag{6}$$

where A is the cross sectional area of the sample gage

section, is displayed along the vertical axis. The crosshead travel, ΔL , which is related to the strain, ϵ , by

$$\epsilon = \frac{\Delta L}{Le} \tag{7}$$

where Le is the effective gage length, is displayed along the horizontal axis. An extensiometer suitable for measuring the small change in the length of a gage section of uniform cross section was not available. Therefore, the absolute value of strain and Young's modulus, E, which is defined by

$$E = \sigma/\epsilon \tag{8}$$

in the elastic range, was not determined. This is no serious disadvantage because the relative values of these properties as a function of filler parameters is of more interest than their absolute values. Since all of the tensile samples were of the same geometry, the effective gage length, Le, should remain constant for all samples. This has been shown to be the case with other polymers [14], and it seems reasonable for this material because there is very little deformation during the test. Based on this assumption, the strain is directly proportional to cross head travel and

$$\frac{\epsilon_1}{\epsilon_2} = \frac{\Delta L1}{\Delta L_2} \tag{9}$$

Based on the same assumption relative modulus can also be determined from the initial slope of the curve shown in Figure 3. This can be shown by combining equations (6), (7), and (8)

$$E = - = \frac{F/A}{L/L_e} = \frac{Le\ F}{A\ \ L} \qquad (10)$$

$$E = (\text{constant}) \times (\text{slope}) \qquad (11)$$

and

$$E/E_o = \frac{\tan\theta}{(\tan\theta)_o} \qquad (12)$$

where θ is defined in Figure 3.

In addition to relative modulus and relative strain the tensile strength and the energy required to break the sample at low strain rate, which is the area curve, can also be determined from the tensile test data.

b - Flexural Test

A Gehman Flex Tester was used to determine the shear modulus, G. Since Young's modulus and the shear modulus are related by (15)

$$E = (1 + \mu)G \qquad (13)$$

where μ is Poissons ratio, this test provides an independent method of determining modulus and a means of verification of the tensile test results.

2 - Thermal Properties

a - Thermal Expansion

A diagram of the experimental setup used in the thermal expansion measurements is shown in Figure 4.

At the start of the test the holder, rod, sample, and furnace are all at room temperature. The sample is placed in the fixture and the rod is adjusted until it is in contact with the sample. The output of the linear voltage differential transformer, LVDT, is adjusted to zero by positioning its core. The furnace heater is then turned on and the sample is heated at a rate of $400\ ^{o}C$ per hour. As the sample expands, the rod pushes the core of the LVDT. The LVDT provides an output voltage which is directly proportional to the displacement of its core. This voltage is displayed on the Transducer Amplifier Indicator and recorded on the chart recorder. The temperature of the sample, which is monitored by means of thermocouples is also recorded on the chart recorder.

The coefficient of linear thermal expansion is defined by (16)

$$\alpha = \frac{\delta L}{L_o (T - T_o)} \qquad (14)$$

α is the linear coefficient of thermal expansion

δL is the change in length of the sample

L_o is the length of the sample at temperature T_o

and

T is the temperature at which δL is measured.

Solving equation (14) for $\delta L/L_o$ yields

$$\delta L/L_o = -\alpha T + \alpha T_o \qquad (15)$$

This is a convenient form of the equation to use because over the temperature range of this experiment $\delta L/L_o$ is a linear function of temperature, and α is a constant which can readily be determined from the slope of the $\delta L/L_o$ versus temperature plot.

Since the sample holder and the rod are of different lengths, their expansion is not the same and a correction is necessary. The holder being longer than the rod, expands on heating more than the rod. This difference in expansion detracts from the apparent change in length of the sample. The apparent change in length of the sample, δL is thus composed of two parts.

$$\delta L = \delta L_s - \delta L_h$$

$$= L_s (- \alpha_s T_o + \alpha_s T) - L_h' (- \alpha_h T_o + \alpha_h T) \qquad (16)$$

where the subscripts s and h refer to the sample and holder respectively. The rod and the holder are both made of fused silica and have the same linear coefficient of thermal expansion. Their difference in expansion is therefore related to the difference in their lengths, and $L_h' = L_s$. Dividing equation (16) by L_s and combining terms yields

$$\frac{\delta L}{L_s} = - A_o + (\alpha_s - \alpha_h) T \qquad (17)$$

where A_o is a constant which is given by

$$A_o = (\alpha_s - \alpha_h)\, T_o \qquad (18)$$

α_h has a value of 0.5×10^{-6} per degree C over a temperature range of 20 to 1000°C, (17) and α_s is given by

$$\alpha_s = 0.5 \times 10^{-6}/^{o}C + \frac{d\left[\frac{\delta L}{L_s}\right]}{d\,T} \qquad (19)$$

b - Linear Mold Shrinkage

Mold shrinkage, which is the shrinkage which occurs as a molded part is cured in the mold and cooled to room temperature can be a problem when molding parts of non-uniform cross section such as a tensile sample. Linear mold shrinkage measurements were made as a function of filler concentration by measuring the length of the Gehman Sample and its mold cavity. The Gehman Sample was used in these measurements for two reasons. First, because of its rectangular shape its shrinkage is unrestricted by the mold cavity. Second, its relatively long length tends to amplify the effect of shrinkage. The Gehman Sample and the corresponding mold cavity were measured with a vernier caliper. The linear mold shrinkage was calculated by

$$S = \frac{L_c - L_s}{L\,c} \qquad (20)$$

where S is the shrinkage.

L_c is the length of the mold cavity.

L_s is the length of the sample.

3 - Electrical Properties

The relative dielectric constant and dissipation factor as a function of filler concentration were determined from measurements made with a General Radio type 1690A dielectric sample holder in conjunction with a General Radio type 1680A capacitance bridge. The sample holder is a two terminal device with circular electrodes which are two inches in diameter. One of the electrodes is fixed and the other is attached to a micrometer adjustment which is calibrated to indicate the spacing between the plates. The bridge is an automatic balance type which provides a digital readout of both capacitance and dissipation factor.

Two measurements are required in order to determine the dielectric constant and dissipation factor. One measurement is made with the sample in the holder. The sample thickness, t_1, the capacitance, C_T, and the dissipation factor, D_1, are recorded. The sample is then removed from the fixture and electrode spacing is adjusted until the capacitance is again equal to C_T. The spacing, t_2, and dissipation factor, D_2, are recorded. From these data and the information in the manufacturer's instruction manual the dielectric constant and dissipation factor are calculated [18].

The dielectric constant and dissipation factor calculations are based on the difference in two readings. Therefore, the stray capacitance, which is assumed to remain

constant during the two measurements, need not be known. This is the chief advantage of this type of dielectric sample holder [19].

4 - Rheological Properties

Flow testing was done with a capillary extrusion rheometer. This instrument, which is supplied as an accessory to the Instron testing machine, has been used to investigate the rheological properties of both thermoplastics [20] and thermosetting plastics [13]. The essential parts of the rheometer are shown schematically in Figure 5. Material which is at room temperature is placed in the heated barrel. If the barrel temperature is sufficiently high, the plastic softens and can be extruded through the capillary tube. The plunger which forces the plastic through the barrel is driven by the Instron cross head. The extrusion rate and thus the shear rate can be varied over a wide range by changing the cross head speed. The force required to extrude the plastic is recorded on a chart recorder which runs at a constant rate. A typical plot of extrusion force versus time for a thermosetting plastic is shown in Figure 2.

Capillary tubes are available with a wide range of length to diameter ratios. In general this ratio should be large (> 30) in order that the energy required for steady flow is large with respect to energy losses due to end effects [20]. With thermosetting material there is an additional factor

to be considered. The material cross-links to varying degrees, depending on the temperature and extrusion rate, during the test, and a solid slug of material remains in the capillary. Difficulty was encountered in removing the slug from the two inch long 0.060 inch diameter capillary used in the initial trial. The slug removal problem was alleviated by using a 0.125 inch long, 0.060 inch diameter capillary, but this low L/D value probably results in errors due to end effects. However, with the short capillary it is possible to make meaningful comparisons between materials and extrusion conditions even though there is doubt as to the absolute accuracy of the measurements.

The shear stress at the capillary wall is related to the pressure drop in capillary by (20)

$$S = \frac{Pr}{2L} \qquad (21)$$

where

S is the shear stress

P is the pressure drop through the capillary

r is the capillary radius

L is the capillary length

Assuming that the pressure drop in the barrel is negliable in comparison to that in the capillary, the pressure drop can be calculated from the extrusion force, F, and the capillary geometry.

$$P = \frac{F}{\pi (r)^2} \qquad (22)$$

Substituting this into (21) yields

$$S = \frac{F}{2 \pi rL} \tag{23}$$

For the .125 inch long, 0.06 inch diameter capillary the shearing stress is

$$S = 42.4\ F \tag{24}$$

with F in pounds, S is in pound per square inch.

The shear rate at the capillary wall is given by (20)

$$D = \frac{4\ Q'}{\pi\ r^3} \tag{25}$$

where

D is the shear rate

Q' is the volumetric flow rate

For the 3/8 inch barrel diameter Q' is give by

$$Q' = \pi/4\ (9/64)\ v \tag{26}$$

where v is the cross head speed. Substituting for the rheometer constants into (25) yields

$$D = 5{,}200\ v \tag{27}$$

with v in the inches per second D has units of $(\text{seconds})^{-1}$.

The apparent viscosity is defined at the ratio of shear stress to the shear rate (20) and can be calculated from the experimental data by using equations (24 and (27)

C - Sample Preparation

1 - Molding Press

The tensile, Gehman and dielectric samples were transfer molded in a three piece mold. The molding press is shown in Figure 6 with the tensile sample mold in place between the platens. The platens are heated by electric heaters and their temperature is controlled by Wheelco controllers in conjunction with saturable core reactors. In addition, the temperature of both top and bottom mold plates is monitored by two iron-constantan thermo-couples and the Daystrom model 6702 temperature recorder. The mold is held closed by the hand operated hydraulic jack which provides a clamping force of 1,500 pounds. The molding compound is forced into the mold cavities by a 1 1/8 inch diameter ram which is accuated by a Miller air cylinder. The ram force, F, is directly proportional to the air pressure, p, and is given by

$$F = 19.6\ (in^2)p \tag{28}$$

with F in pounds and p in pounds per square inch [21].

2 - Mold

The mold is shown in Figure 7. It consists of top and bottom plates which can be used with either of the three inserts. The bottom plate has two locating pins to keep the assembled mold aligned. The top plate has a hole through which the compound passes and a runner which is half circular in cross section. With the Gehman and dielectric inserts

half-circular runner serves as the entire runner system, but with the tensile sample insert there is a similar half circular runner with mates with the one in the top plate to for a 1/8 inch diameter circular runner system.

3 - Sample Configuration

The molded test samples are shown in Figure 8. Because of the limited amount of material available the large ASTM-type 1 tensile sample was not used [22]. The sample which was used is similar to that recommended for use by Karnowsky and Colp[23] when material economy is important. This sample differs from that recommended by Karnowsky and Colp in two ways: (1) It is an inch shorter. (2) It is 1/8 inch thick; their sample is 1/4 inch thick. Both of these changes were made in order to conserve material.

The dimensions of the dielectric sample were determined in accordance with the requirements stated in the operating instructions for the sample holder [18]. First, the thickness of the sample should be such that the capacitance with the sample in the holder is 20 to 70 pf. This insures that holder is operated in its most accurate range. For a value of 50 pf the thickness is given by

$$t = 14.1\ k \tag{29}$$

where

t = sample thickness in mils

k = relative dielectric constant of the material to be tested.

Using a value of $k = 3.4$[24] the value of t is approximately 50 mils. Second, in order to reduce the effect of fringing the sample diameter should be less than the diameter of the electrodes by 5 t. Therefore, the sample mold cavity diameter is

$$D = 2.0 \text{ in.} - 5(.05 \text{ in.}) = 1.75 \text{ in.}$$

The Gehman sample is 4 in. long, 0.31 in. wide, and 0.033 in. thick.[30] The relatively small cross-sectional area was chosen to reduce the force required for flexure. The actual test specimen is two inches long and are obtained by scribing and breaking the four inch bars in half.

The sample, used in the measurement of the coefficient of linear thermal expansion, is 1/8 inch in diameter and approximately 1.4 inches long. These specimens were obtained from the straight section of the tensile sample mold runner.

4 - Molding Conditions

Where possible, all samples were molded at 350°F with a ram force of 785 pounds and cured in the mold under pressure for four minutes. The exceptions to these conditions are as follows:

(1) Because of excessive mold shrinkage which resulted in fracture in the mold when molded under the above conditions, tensile samples from the Group #2 material with $V_f = 0.06$ were molded a T = 325°F, F = 785 lbs. and t = 3 min.

(2) Because of the high viscosity of the Group #2 material with V_f = 0.70 the ram force was increased to 1,650 pounds for all samples in order to fill the mold cavity.

All samples were given a two hour post cure at 400°F in a forced air oven.

5 - Preform Pellets

To facilitate handling preformed pellets were made from the powderd material for both molding and rheometer applications. The molding preforms were one inch in diameter and weighed approximately 15 grams; the rheometer preforms were 3/8 inches in diameter and weighed approximately 4.2 grams. The preforms for both applications were dry pressed in cylinderical die with an applied force of 4,000 pounds.

Difficulty was encountered in making preforms from the Group #2 material which had filler volume concentrations less than 57%. For these samples, the material was used in powder form for molding and the rheometer experiments.

III - RESULTS AND DISCUSSION

A - Mechanical Properties vs. Filler Concentration

1 - Tensile Strength

The results of the tensile tests which were performed on the material with variable filler concentration are summarized in Table 1. The tensile strength at break, which is plotted in Figure 9, increases to a value which is approximately two and one half times that of the unfilled resin as the filler concentration is increased to seventy percent by volume. This increase in tensile strength is not common to all polymer-filler systems. For example, a decrease in the tensile strength of epoxy resins with increasing limestone filler concentrations have been reported [25]. Cohan[3] found that the tensile strength of natural rubber increases to a maximum and then decreases as the concentration of the calcium carbonate filler is increased. Neisen[8], in summarizing the theories of tensile behavior of filled polymers, shows that theoretically tensile strength may either increase, decrease, or remain substantially constant as filler concentration is increased. This vast difference in behavior is attributed to the difference in adhesion between polymer and filler which changes greatly from one filler, polymer system to another. The magnitude of the increase in tensile strength indicates that there is adhesion between the resin and filler

in this system.

2 - Modulus

The relative tensile modulus, E/E_o, was determined from the initial of slope of Instron tensile test curve as shown in Figure 3. A value of tan θ for each of the samples was determined. The value of $(\tan \theta)_o$, which is the slope of the tensile curve for the unfilled resin, was found as shown in Figure 10 by extrapolating the curve to zero filler. E/E_o was calculated by

$$E/E_o = \frac{\tan \theta}{0.85} \qquad (12\text{-A})$$

The modulus was also measured with a Gehman Flex Tester. By assuming a value of 0.5 for Poisson's ratio which is a good approximation for rubbery materials,(15) Young's modulus, from (13), is given by

$$E = 3G \qquad (13\text{-A})$$

The values of E calculated from the results of Gehman test are shown in Table 1 and plotted in Figure 11.

E/E_o for both the tensile and flexural test are shown in Figure 12. While there is a significant difference in the results for the two methods, both show a substantial increase in modulus with filler concentration. At $V_f = 0.7$, E/E_o is 3.5 and 7.9 respectively. The reasons for the difference in these values is not clearly understood. It could result from the difference in the geometry of the samples used in the two

tests or from other experimental factors.

Also shown in Figure 12 are the theoretical curves according to Guth's equation[2]

$$E/E_o = 1 + 2.5\ V_f + 14.1\ V_f^2 \qquad (2\text{-A})$$

and the modified Eilers-Van Dijck equation [8]

$$E/E_o = \left(\frac{1 + 1.25\ V_f}{1 - KV_f} \right)^2 \qquad (31)$$

with the value of K = 0.5. Both curves have the same general shape as the experimental data. The better fit is obtained with equation (31).

3 - Apparent Elongation

The apparent elongation, which is the distance the Instron crosshead moves during the tensile test, is tabulated in Table 1. This function, which is linearly related to the ultimate elongation (or strain) of the material, is a somewhat erratic function of the filler concentration, but does follow a decreasing trend as the filler concentration is increased. To a first approximation the elongation can be represented as a linear function of V_f. This is shown in Figure 13 where the data are plotted along with the line representing the linear least squares fit of the data.

4 - Energy to Fracture

The energy required to fracture the tensile samples at a low strain rate was calculated from the area under the tensile test curve. The area was evaluated by tracing the Instron

curves on mylar tracing paper, cutting out the area and weighing it on a micro balance. From the weight and density of the tracing paper sample and scale factors from the Instron machine, the energy required to fracture, ξ, can be calculated.

ξ as a function of filler concentration is shown in Figure 14. At the lower values of V_f both E and tensile strength increase and the elongation decreases. The net effect is an increase in the area under the curve with increasing filler concentration. This trend continues until V_f reaches a value of approximatly 0.6 where ξ reaches its maximum value. As V_f is increased from 0.63 to 0.70 the increase in E and the tensile strength is more than off set by the decrease in elongation and the net result is a slight decrease in ξ. However, since the maximum in the ξ vs. V_f curve is rather broad, the change in ξ at concentrations greater than 50% filler are almost insignificant.

B - Mechanical Properties vs. Filler Particle Size Distribution

Particle size measurements were made on samples of the standard filler and the three groups which were separated from the standard filler, as described in Appendix 2. The resulting size distributions are plotted in Figure 15 for the standard filler and in Figure 16 for the especially prepared distributions.

The results of tensile tests performed on the Group #3 material are summarized in Table 2. The volume fraction of filler

was determined by making density measurements as described in Appendix 1 and found to be 0.63 which corresponds to one of the Group #2 samples. Data on this sample, indicated in Table 2 as having standard filler distribution, are shown for comparison. The difference in the tensile properties of the samples with variable filler particle size distributions is not significent.

This experiment was performed with particle diameters, d, ranging from 9μ to 24μ .* The apparant lack of agreement between the results of this experiment and those reported by Alter[10] and Warrick[11] are probably due to two factors:

(1) The range of particle diameter is so small compared to that of Warrick (5 to 150 mμ) that the particle size effect is not significant.

(2) The reinforcing effect of fillers with diameters in the range available here is not as great as those with diameters less than 50 mμ .[26]

C - Thermal Properties

1 - Thermal Expansion

Linear thermal expansion measurements were made on each of of the seven Group #2 samples in the 25^{o} to 250^{o}C temperature range. The normalized increase in length is shown in Figure 17.

---

* In the "fine" distribution 50% by volume have diameters less than 9μ ; in the "coarse" distribution 50% by volume have diameters less than 24μ (Figure 16).

The magnitude of the thermal expansion decreases significantly with V_f. For each of the samples, the normalized change in length, $\frac{\delta L}{L}$, can be very closely approximated by a linear function of temperature. The coefficient of linear thermal expansion as calculated from the slope of the lines by the following equation

$$\alpha = 0.5 \times 10^{-6}/^{o}C + \frac{d\left(\frac{\delta L}{L}\right)}{dT} \qquad (19)$$

where the constant term is the calculated correction for the sample holder, decreases approximatly six fold as V_f is increased to 0.7.

The thermal expansion of a composite system consisting polyurethane rubber and sodium chloride filler was investigated by Van-Der Wal, Bree and Schwargl.[27] They found that the coefficient of volume thermal expansion for their system obeyed a simple linear relation which can be derived for the two component system by assuming that each component can expand without being restricted by the other member. The change in volume of each component is given by

$$\Delta v_i = A_i v_i \Delta T \qquad (32)$$

where

v_i is change in volume of the i^{th} component

A_i is the coefficient of thermal expansion and

v_i is the initial volume of the i^{th} component

ΔT is the change in temperature

The total change in volume, Δv, is simply the sum of the volume changes of the components. For the resin filler notation

$$\Delta v = (A_r v_r + A_f v_f)\,\Delta T \tag{33}$$

Dividing (33) by the initial volume, v_o, and ΔT yields

$$A = \frac{v}{v_o \Delta T} = \frac{A_r v_r}{v_o} + A_f \frac{v_f}{v_o} \tag{34}$$

where A is the volume expansion coefficient for the composite material. For the two component system

$$\frac{v_r}{v_o} = V_r \tag{35}$$

and

$$\frac{v_f}{v_o} = V_f \tag{36}$$

where V_r and V_f are the volume fractions of resin and filler respectively at the initial temperature. Equation (34) can be further simplified by

$$V_r = 1 - V_f \tag{37}$$

and

$$A = A_r + (A_f - A_r)V_f \tag{34-A}$$

This result can be related to linear thermal expansion by dividing (34-A) by 3 and noting that[28]

$$\frac{A_i}{3} = \alpha_i \tag{38}$$

In terms of linear coefficients the expression becomes

$$\alpha = \alpha_r + (\alpha_f - \alpha_r)V_f \tag{34-B}$$

From the literature, the coefficient of linear thermal expansion for the fused silica filler is $0.5 \times 10^{-6}/^{o}C$.[17] A value of $160 \times 10^{-6}/^{o}C$ was estimated for α_r by extrapolation of the experimental data to zero filler concentration. Since $\alpha_r \gg \alpha_f$ (34-B) becomes

$$\alpha \simeq \alpha_r(1 - V_f) \qquad (34\text{-C})$$

α from experimental data and equation (34-C) with $\alpha_r = 16 \times 10^{-5}/^{o}C$, are shown in Figure 18. From this graph it is evident that the experimental values of α are lower than predicted by (34-C). While this model yields good results with the rigid filler (NaCl) in the soft matrix (polyurethane rubber),[27] it is inadequate for the silicone molding compound, where both filler and resin are rigid. Since both components are rigid, their expansion is restricted and a lower expansion coefficient than predicted by (34-C) results.

A more complex expression for the thermal expansion coefficient was proposed by Kerner.[27] In his formula the mutual restrictions to expansion which the components impose on each other are considered. Kerner's equation for this system is

$$\alpha = \alpha_r + (\alpha_f - \alpha_r)V_f + (\alpha_f - \alpha_r)(V_f - V_f^2)f \qquad (39)$$

where

$$f = \frac{\frac{1}{Br} - \frac{1}{Bf}}{\frac{(1-V_f)}{B_f} + \frac{V_f}{B_r} + \frac{3}{4G_r}} \qquad (40)$$

and

B_r and B_f are bulk modulus of resin and filler respectively and G_r is the shear modulus of the resin

All the terms in (40) are material constants except V_f, and the expression can be reduced to

$$f = \frac{1}{V_f + k'} \qquad (40\text{-A})$$

where k is a dimensionless constant given by

$$k' = \frac{B_r}{B_r - B_f} + \frac{B_r}{G_r} \left[\frac{3B_f}{4(B_r - B_f)}\right] \qquad (41)$$

Substituting (40-A) into (39) and again noting that for this material $\alpha_r \gg \alpha_f$, equation (39) becomes

$$\alpha \simeq \frac{\alpha_r k'(1-V_f)}{V_f + k'} \qquad (39\text{-A})$$

α as calculated from equation (39-A) with $k' = 0.85$ and $\alpha_r = 16 \times 10^{-5}/^{o}C$, is also shown in Figure 14. The calculated results agree very closely with the experimental values of α.

If a system follows the simple linear model which allows the unrestricted expansion and contraction of each component with temperature, the resulting material would be essentially free from internal stress. With this system there is a rather

large deviation from linearity, and it is reasonable to assume that a high residual stress results. If it is assumed that the composite material is free from residual stress at the elevated molding or post cure temperature, the resin is placed in tension and the filler in compression as the temperature is lowered. These residual stresses may alter the overall properties of the material and be at least partially responsible for the extreme brittleness of the material.

2 - Linear Mold Shrinkage

An object molded from the silicone molding compound is smaller than its mold cavity. This shrinkage, which is referred to here as mold shrinkage and as linear mold shrinkage when only one dimension is considered, is the result of two factors:

(1) A reversible component of shrinkage which is caused by cooling the molded object from the molding temperature to room temperature.

(2) A irreversible component which is due to the chemical reaction which occurs during cureing.

The reversible component can be calculated by

$$\left(\frac{\delta L}{L}\right)_{rev.} = \alpha (T_o - T_m)$$

where α is coefficient of linear thermal expansion

T_o is room temperature

and T_m is the molding temperature of 178^oC

The total linear mold shrinkage was determined experimentally. The irreversible component was determined by subtracting the reversible shrinkage from the total shrinkage.

The experimentally determined linear mold shrinkage at a molding temperature of 350°F along with the calculated reversible and irreversible components are shown in Figure 19. The total shrinkage decreases substantially as V_f is increased. The irreversible shrinkage with the exception of the point at $V_f = 0.41$, decreases linearly with V_f; or stated another way it increases linearly with V_r. The discrepancy at $V_f = 0.41$ can probably be attributed to experimental error since the corresponding point for total shrinkage is also out of line with its neighboring points. In general, a low mold shrinkage is an advantage. This is especially true when complex shapes which do not allow unrestricted shrinkage are molded.

D - Dielectric Constant and Dissipation Factor vs. Filler Concentration

The relative dielectric constant and dissipation factor for the range of filler concentrations were measured at 400HZ. These measurements were made on the samples in the "as molded" condition and after post cure. The data are shown in Table 3.

Both the dielectric constant and the dissipation factor decrease during post cure. The dissipation factor decreased by approximately 50%; the decrease in the dielectric constant is on the order of 5 to 10%.

The dissipation factor does not follow any particular trend as filler concentration is increased. This may be due largely to experimental inaccuracies which arise from the fact that the losses within the material are so small that the dissipation factor can not be accurately measured with the available equipment. As a result of these uncertainties the only significant fact that can be learned from the dissipation factor measurements is that it decreases substantially during the post cure treatment.

As shown in Figure 17, the dielectric constant in both the "as molded" and post cured conditions increase approximately linearly with V_f. However, the increase in each condition is less than 25% and this is insignificant in most applications. Looyena [29] derived an equation for the dielectric constant of a composite material. His equation, which was found to accurately describe the behavior of a mixture of glass spheres in carbon teirachloride is

$$k = \left[(k_f^{1/3} - k_r^{1/3}) V_f + k_r^{1/3} \right]^3 \qquad (43)$$

where k, k_r and k_f are the relative dielectric constant of the composite, resin and filler respectively and V_f is volume fraction filler.

To check the general fit of this equation to the experimental data a value of $k_f = 3.78$ [30] was used. Since no data on the dielectric constant of the resin are available, a value of

k_r = 3.0 was extimated from the experimental data. The solid curve in Figure 20 was plotted from equation (43) using these values. This curve follows the same general trend as the experimental data.

E - Rheological Properties

Material from each of the three groups was used in the flow tests. The standard material from Group #1 was used to investigate the effect of temperature and shear rate on flow perperties. The Group #2 and Group #3 materials were used to investigate the effect of filler concentration and filler particle size distribution on the rheological behavior.

1 - Temperature Effect

In order to determine the effect of temperature on the minimum shear stress and hardening time, a number of runs were made at a constant shear rate with the Group #1 material. Each run was made with two preformed pellets having a mass of 4.2 gm each. The Instron cross head was set at a speed of one inch per minute. The resulting shear rate, as given by (27) was

$$D = 86.8 \text{ (sec.)}^{-1}$$

The runs were made at temperatures ranging from 225° to 325°F. Testing was limited to this temperature range because: (1) at temperatures greater than 325°F the material hardened so rapidly and nonuniformly that the capillary became blocked, (2) at

temperatures below 225° the shear stress and hardening time both are excessive and the test is impractical.

The minimum shear stress S_o decreases with temperature as shown in Figure 21. Each point represents the average of the data from two to four runs. The minimum shear stress is calculated from the experimental data by applying equation (24) to the corrected minimum force from the Instron chart recorder. The correction is made by adding the weight of the plunger, which is approximately one pound, to the minimum force, F_o, as indicated in Figure 2. This curve is also proportional to the minimum apparant viscosity since the shear rate is constant.

S/S_o as a function of temperature is shown in Figure 22. These curves represent the normalized average behavior of the material. No attempt was made to show the shape of the curves during the melting or to show the erratic variations in S which occur during extrusion due to nonuniform hardening.

The time required for the minimum shear stress to increased by a fixed proportion (for example to double) is a measure of the hardening rate of the material. (See Figure 2). The recropocal of this time, $1/t(x)$, and the absolute temperature, T, are related by the well known Arrhenius relationship

$$1/t(x) = A \exp(-Q/RT) \qquad (44)$$

where A is a constant

Q is the "apparent" activation energy

R is the gas constant

Q is found from the experimental curves by taking the logarithm of (44)

$$\ln \quad 1/t(x) \quad = \ln A - \frac{Q}{RT}$$

which is a linear expression in 1/T. A plot on semilog paper of 1/t(x) for S/S_o = 1.5 and 2.0 versus 1/T is shown in Figure 23. The values of Q for these plots as determined by the slope of the least squares line are:

at $S/S_o = 1.5$; $Q(1.5) = 7.0 \frac{\text{killo cal.}}{\text{mole}}$

and

at $S/S_o = 2$; $Q(2.0) = 7.9 \frac{\text{killo cal.}}{\text{mole}}$

The values of the "apparent" activation energy are empirically determined constants which are used to relate the hardening time and the absolute temperature. While they are related to the activation energy of the cross-linking reaction, there is insufficient information available to allow quantitative judgements.

2 - The Effect of Shear Rate

The minimum shear stress as a function of shear rate is shown in Figure 24. These data were obtained by making a number of runs at 300°F with different Instron cross head speeds. The linear plot on log, log paper indicates a power relationship between S_o and D.

This relationship as determined from the experimental data is

$$S_o = 170\ D^{0.35} \tag{46}$$

Similar shear rate dependance has been reported for polyethylene and polystyrene.[20]

3 - The Effect of Filler Concentration

The measurement of the flow properties as a function of filler concentration was difficult because the materials with $V_f > 0.57$ could not be readily formed into pellets. Measurements, therefore, had to be made using the material in the powder form. With the powder the melting and flow behavior was somewhat more erratic than with the pellets. Also, it was more difficult to remove the remaining material from the reheometer barrel when the powder was used. Cleaning the barrel was especially difficult when the materials with the lower filler concentration were used. The cleaning problem was lessened by spraying the barrel and capillary with an aerosol mold release agent (Rawleigh RM #606571).

Initial runs with the powdered material indicated that the results varied with the amount of material charged into the barrel. In order to approximate a constant volume of charge the mass of the charge was increased in proportion to the density of the molded material by

$$M = \frac{\rho}{1.31\ gm/cm^3} \times 7gm \tag{47}$$

where 1.31 gm/cm^3 is the molded density of the material with 6% by volume filler.

The minimum shear stress as a function of filler concentration at 250°F and 300°F is shown in Figure 25. Three additional points, which were obtained from tests on pellets of the highly filled materials at 300°F are also shown to illustrate the difference in results when pellets are used.

Two characteristics of the curves are surprising. The first is the rapid increase in S_o as the filler concentration is increased from 63% to 70% by volume; the second is the fact that a greater force is required to extrude the material with $V_f < 0.6$ at 300°F than at 250°F. The rapid increase in S_o above 63% concentration probably results from the fact volume fraction of filler is approaching the theoretical density of uniform close packed spheres which is ~ 74%. At these concentrations the filler particles are in contact with each other and the resin occupies the voids between particles. The friction, that results from the particles being in direct contact, causes a sharp increase in the required shear stress. The second phenomenon may be due to the faster hardening of the material at the higher temperature. This could raise S_o for two reasons:

(1) The hardened material which adheres to the walls of the barrel increase the barrel friction and make the calculated value of S_o greater than it actually is.

(2) An actual increase in S_o due to the increased hardening rate at 300°F.

The time required for the minimum shear stress (and apparent viscosity) to increase to a value which is two times the minimum as a function of filler concentration at 300°F is shown in Figure 26. This plot shows that the increased filler concentration decreases the hardening rate of the material.

4 - The Effect of Particle Size Distribution

The minimum shear stress and the time required for S/S_o to reach a value of 2 at 300°F and a shear rate of 86.8 $(sec)^{-1}$ is shown in Table 4. Both S_o and t(2) increase as the fraction of "fine" particles is increased.

There appears to be an interaction between the resin and filler during the hardening reaction which decreases the hardening rate, and this decrease is proportional to the surface area of the filler. This is shown in Table 4 where the increase in surface area is due to a decrease in particle size and in Figure 24 where the increase in surface area is due to an increased filler concentration.

IV - CONCLUSIONS

The overall balance of mechanical properties of the silicone resin molding compound is enhanced by increasing the filler concentration. This is reflected by a $2\frac{1}{2}$ fold increase in tensile strength and a 2 fold increase in the energy required to fracture, or toughness, as the filler concentration goes from zero to 70% by volume. This increase in filler concentration is also accompanied by a significant increase in the modulus and a slight decrease in ultimate elongation. The higher modulus is not always an advantage, but it is necessary in order to obtain the higher tensile strength and toughness. The decrease in ultimate elongation is undesirable, but a five to ten percent decrease in its value must be tolerated in order to gain the advantage of the higher tensile strength and toughness.

The coefficient of thermal expansion decreases to a value which is approximately one fifth that of the unfilled resin as the filler concentration is increased to 70% by volume. This decrease in thermal expansion is an advantage in applications where it is used in conjunction with metals. However, even with $V_f = 0.7$, the coefficient of linear thermal expansion is on the order of twice that of most metals. The mechanical properties are not significantly affected by changes in the filler particle size distribution within the relatively narrow range of particle diameters available for this experiment (9 to 24 μ).

The dielectric constant increases with filler concentration. However, this increase is slight and is not an important factor in most applications.

The minimum apparent viscosity is not a very strong function of concentration at filler volume fractions below 0.63. However, it increases sharply as V_f is increased to 0.70. This increase in viscosity, which is probably due to direct contact between the filler particles, makes transfer molding very difficult at filler concentrations greater than 63%.

The effect of temperature and shear rate on the flow properties were investigated at only one filler concentration ($V_f = 0.63$). For this material at $300^{o}F$ the minimum shear stress, S_o, is related to the shear, D, by

$$S_o = 170\ D^{0.35}$$

The shear stress, at a shear rate of 86.8 $(\text{seconds})^{-1}$, decrease substantially with temperature.

The hardening rate, and the absolute temperature at a shear rate 86.8 $(\text{seconds})^{-1}$ are related by

$$1/t(2) = A \exp\left(\frac{-7.9 \times 10^3 \text{ cal/mole}}{RT}\right)$$

where t(2) is the time, in seconds, required for the viscosity to reach a value which is twice the minimum.

In view of these factors, the best resin filler combination for most applications is that which has 63%, by volume, filler. From the standpoint of mechanical properties the material with 70%, by

volume, filler is better because of its higher strength and lower coefficient of thermal expansion. However, because of the difficulty of molding this material it is impractical in most applications.

APPENDIX I

Calculation of Volume Concentration of Filler from Mass Concentration Data

Most of the data on filler phenomena in plastics found in the literature are presented with the volume concentration or volume fraction of filler as the parameter of interest. The filler concentration in the especially prepared material is given in terms of concentration by mass. In order to make comparisons with the data in literature on other systems it is desirable to know the filler volume fraction. This can be determined in the following manner. Assuming an ideal mixture

$$v = v_f + v_r \tag{48}$$

where v is the total volume and v_f and v_r are the filler and resin volumes respectively. v_f and v_r can be expressed in terms of their respective masses and densities and (48) becomes

$$v = \frac{m_f}{\rho_f} \quad \frac{m_r}{\rho_f} \tag{49}$$

where m is mass and ρ is the density. Dividing (49) by the total mass (m) yields

$$\frac{v}{m} = \frac{m_f}{m}\left(\frac{1}{\rho_f}\right) + \frac{m_r}{m}\left(\frac{1}{\rho_r}\right) \tag{50}$$

or

$$\frac{1}{\rho} = \frac{M_f}{\rho_f} + \frac{M_r}{\rho_r} \tag{51}$$

where M_f ($=\frac{m_f}{m}$) and M_r ($=\frac{m_r}{m}$) are the mass fractions of filler and resin respectively and ρ is the compound density. For the two component system

$$M_r = 1 - M_f \tag{52}$$

Substituting this into (51) and simplifying yields

$$1/\rho = \frac{1}{\rho_r} - \frac{(\rho_f - \rho_r)}{\rho_f \rho_r} M_f \tag{53}$$

The resin and filler densities were experimentally determined by measuring the compound density as a function of filler mass fraction. The density measurements were made on the disc used in the dielectric measurements. Their volume was determined by measuring the diameter and thickness with a vernier caliper; mass was measured on a Mettler micro-balance. The reciprocal density versus mass fraction is shown in Figure 27. Extending the least squares line to filler concentrations of zero and 100% the resin and filler density can be determined:

at $M_f = 0$

$$1/\rho = 1/\rho_r = 0.801 \text{ cm}^3/\text{gm}$$

and

$$\rho_r = 1.25 \text{ gm/cm}^3$$

at $M_f = 1$

$$1/\rho = 1/\rho_f = 0.4607 \text{ cm}^3/\text{gm}$$

and

$$\rho_f = 2.17 \text{ gm/cm}^3$$

This value of ρ_f is in range given for amorphous SiO_2 given in the literature[31].

Substituting these values into equation (53) and taking the reciprocal gives

$$\rho = \frac{1.25 \text{ gm/cm}^3}{1-0.424\ M_f} \tag{54}$$

Once the density has been determined the volume fraction of filler can be calculated by the following method.

$$V_f = \frac{v_f}{v} \tag{55}$$

where

V_f is volume fraction of filler

v_f is the volume of filler in the sample of interest

v is the total volume of the sample

In terms of mass and density the filler volume can be expressed by

$$v_f = \frac{m_f}{\rho_f} \tag{56}$$

and

$$V_f = \frac{m_f}{v\rho_f} \tag{57}$$

Multiplying numerator and denominator by the total mass and identifying terms yields

$$V_f = (\frac{m}{v})(\frac{m_f}{m})(\frac{1}{\rho_f}) = \frac{\rho}{\rho_f}\ M_f \tag{58}$$

Substituting the value of ρ_f and (54) for ρ yields

$$V_f = \frac{0.576\ M_f}{1-0.424\ M_f} \tag{59}$$

The mass fraction filler, the volume fraction filler, calculated by (59) and the density, calculated by (54) are tabulated in Table 5 for the Group #2 material with variable filler concentration.

APPENDIX II

Filler Particle Size Measurements

The distribution of filler particle diameters which are shown in Figures 16 and 17 were determined using A M-S-A Particle Size Analyzer. This equipment and its operation are described in reference (31).

The feeding liquid was a mixture of Acetone (150 ml) and deionized water (350 ml). The sedimentation liquid was 0.1% calgon in deionized water and had a measured density of 0.966 gm/cm^3 and a viscosity of 0.0099 poise at room temperature. A sedimentation capillary with a 75mm diameter was used. The density of the silical filler was taken to be 2.20 gm/cm^3.(30) Using these constants, particle size measurements were made in accordance with reference (31).

TABLE I

TENSILE PROPERTIES VS. FILLER CONCENTRATION

(a) Volume Fraction Filler	(a) Density	Number of Samples Tested	Av. Tensile Strength	Max. Tensile Strength	Std. Dev. of Tensile Strength	Modulus (Gehman) x 10^{-5}	E/E_o (Tensile)	E/E_o (Gehman)	Fracture Energy	Apparent Elongation
--	(gm/cm^3)	--	(lb/in^2)	(lb/in^2)	(lb/in^2)	(lb/in^2)	--	--	(in-lb)	(in)
0	1.25	0	2,030(b)	--	--	2.40(c)	1.0	1.0	0.56(d)	
0.06	1.31	7	2,071	2,253	135	2.82	1.1	1.2	0.57	0.024
0.16	1.40	8	2,183	2,349	159	3.72	1.3	1.5	0.59	0.021
0.28	1.51	8	2,839	3,155	160	6.08	1.8	2.5	0.73	0.019
0.41	1.63	8	3,641	4,088	355	8.10	2.5	3.4	0.95	0.020
0.57	1.71	8	4,852	5,002	167	11.9	3.6	5.0	1.20	0.020
0.63	1.83	8	5,239	5,649	324	14.6	3.7	6.1	1.20	0.022
0.70	1.89	8	5,251	5,703	381	19.0	3.5	7.9	1.10	0.018

(a) - From Appendix 1
(b) - Extrapolated from Figure 9
(c) - Extrapolated from Figure 13
(d) - Extrapolated from Figure 14

TABLE 2

TENSILE PROPERTIES vs. FILLER PARTICLE SIZE DISTRIBUTION

Filler Distribution	Density	Number of Samples	AV. Tensile Strength	Max. Tensile Strength	Std. Dev. of Tensile Strength	E/ Eo (Tensile)	Apparant Elongation	Fracture Energy
-	(gm/cm^3)	-	(lb/in^2)	(lb/in^2)	(lb/in^2)	-	(in)	(in-lb)
STD	1.83	8	5,239	5,649	324	3.74	0.022	1.20
FINE	1.84	8	4,890	5,266	267	3.95	0.014	0.95
MED.	1.84	8	4,395	5,000	364	4.26	0.014	0.80
COARSE	1.84	8	4,486	4,910	280	3.65	0.016	0.77

TABLE 3

DIELECTRIC PROPERTIES vs. FILLER CONCENTRATION

	Relative Dielectric Constant		Dissipation Factor	
Vf	As Molded	After Post Cure	As Molded	After Post Cure
0.06	3.00	3.08	.0042	.0018
0.16	3.29	3.14	.0036	.0016
0.28	3.36	3.06	.0034	.0017
0.41	3.49	3.17	.0038	.0018
0.57	3.62	3.48	.0034	.0020
0.63	3.61	3.41	.0034	.0019
0.70	3.72	3.44	.0040	.0020

TABLE 4

THE EFFECT OF FILLER PARTICLE SIZE DISTRIBUTION ON FLOW PROPERTIES AT T = 300°F AND D = 86.8(sec)$^{-1}$

Filler Distribution	So (lb/in^2)	t(2) (seconds)
FINE	1,840	156
MED.	1,270	145
COARSE	1,210	85

TABLE 5

Group #2 Material

Lot No.	M_f	(gm/cm^3)	V_f
AF-254-L	0.10	1.31	0.060
AF-255-L	0.25	1.40	0.161
AF-256-L	0.40	1.51	0.278
AF-257-L	0.55	1.63	0.413
AF-258-L	0.70	1.71	0.573
AF-259-L	0.75	1.83	0.633
AF-262-L	0.80	1.89	0.697

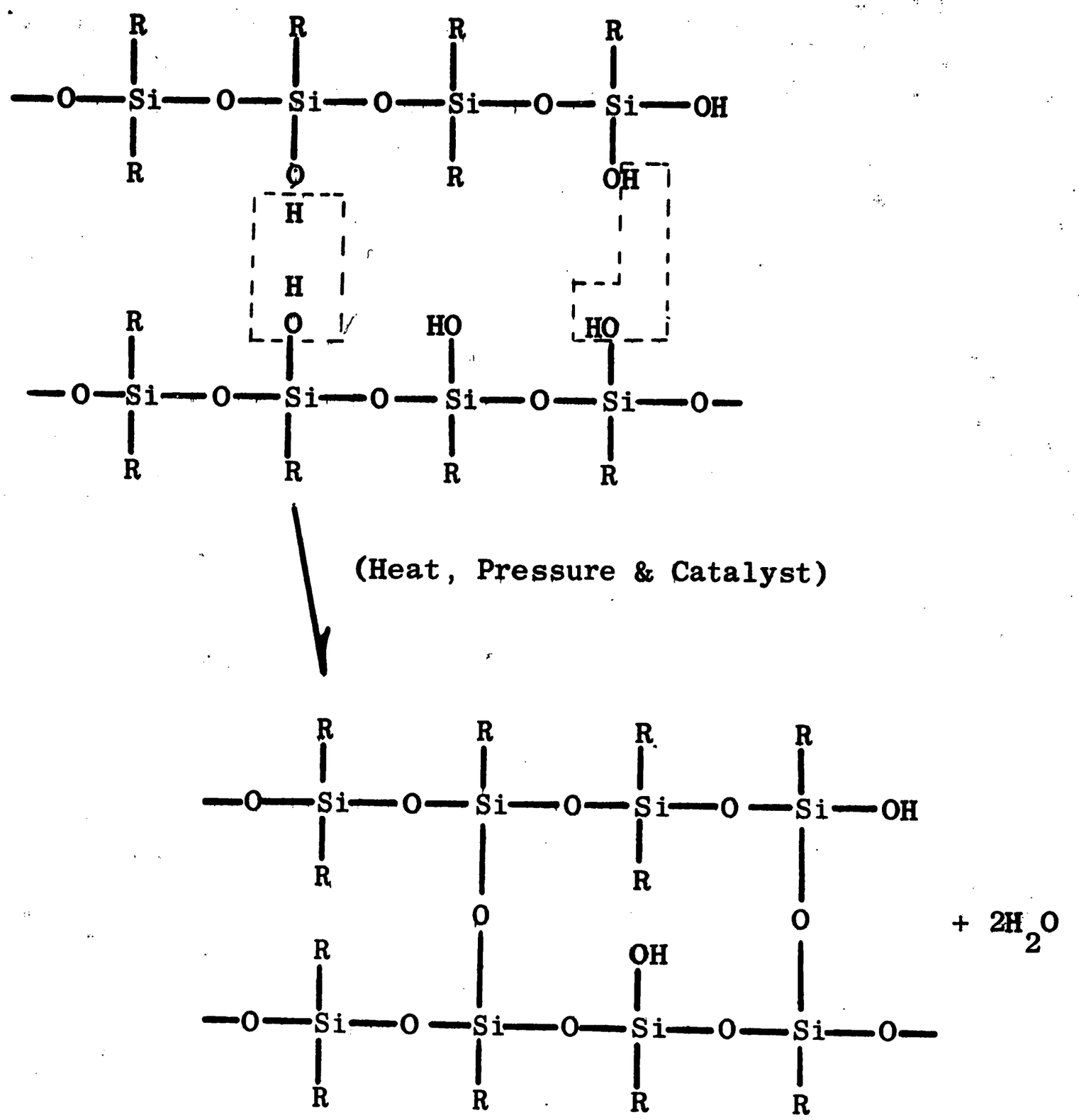

R = Organic Group (s)

FIGURE 1. STRUCTURE OF A TYPICAL SILICONE RESIN ILLUSTRATING THE CURING REACTION (from Ref. 1)

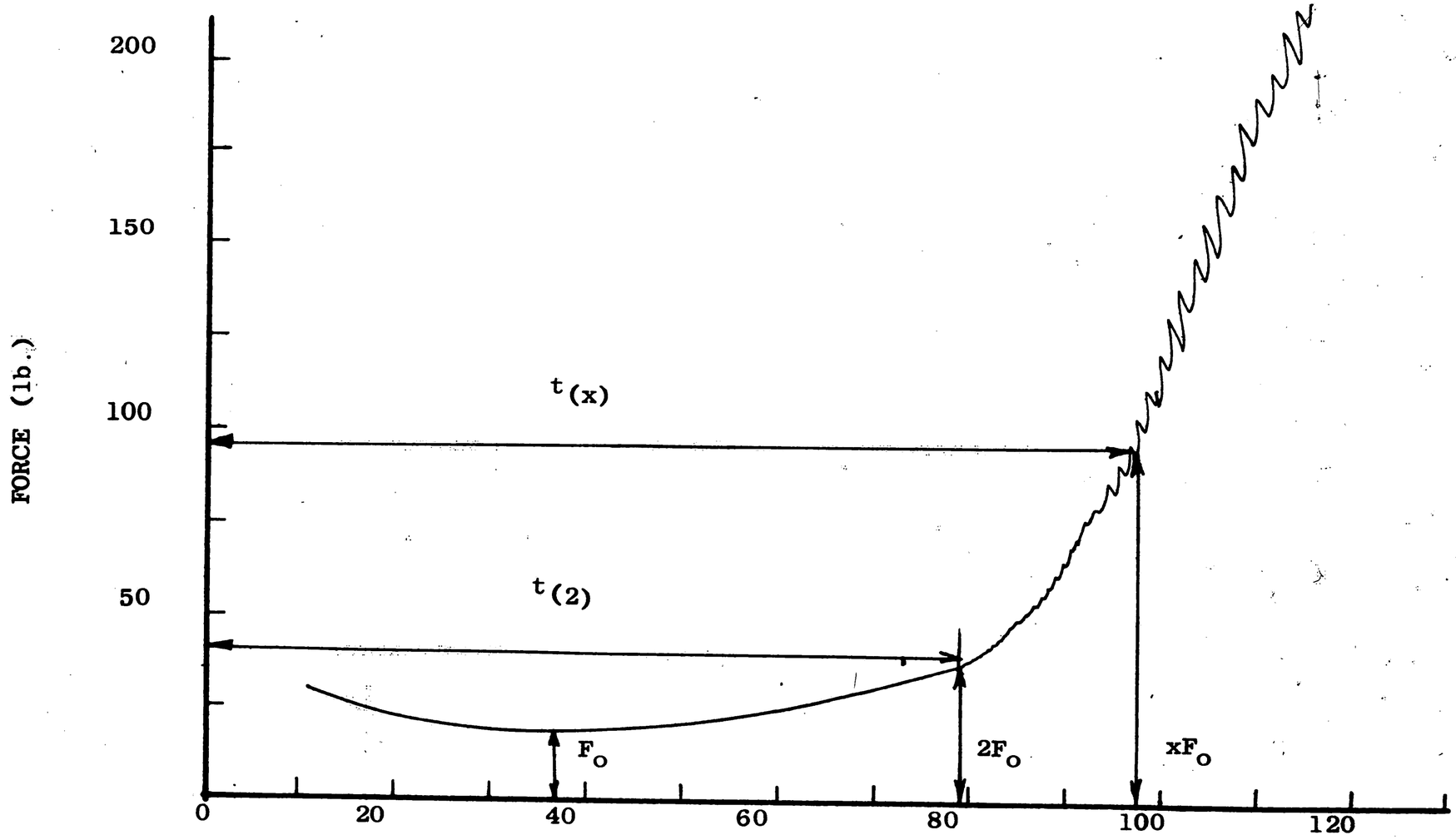

FIGURE 2. TYPICAL PROFILE FROM EXTRUSION RHEOMETER WITH SILICONE RESIN MOLDING COMPOUND

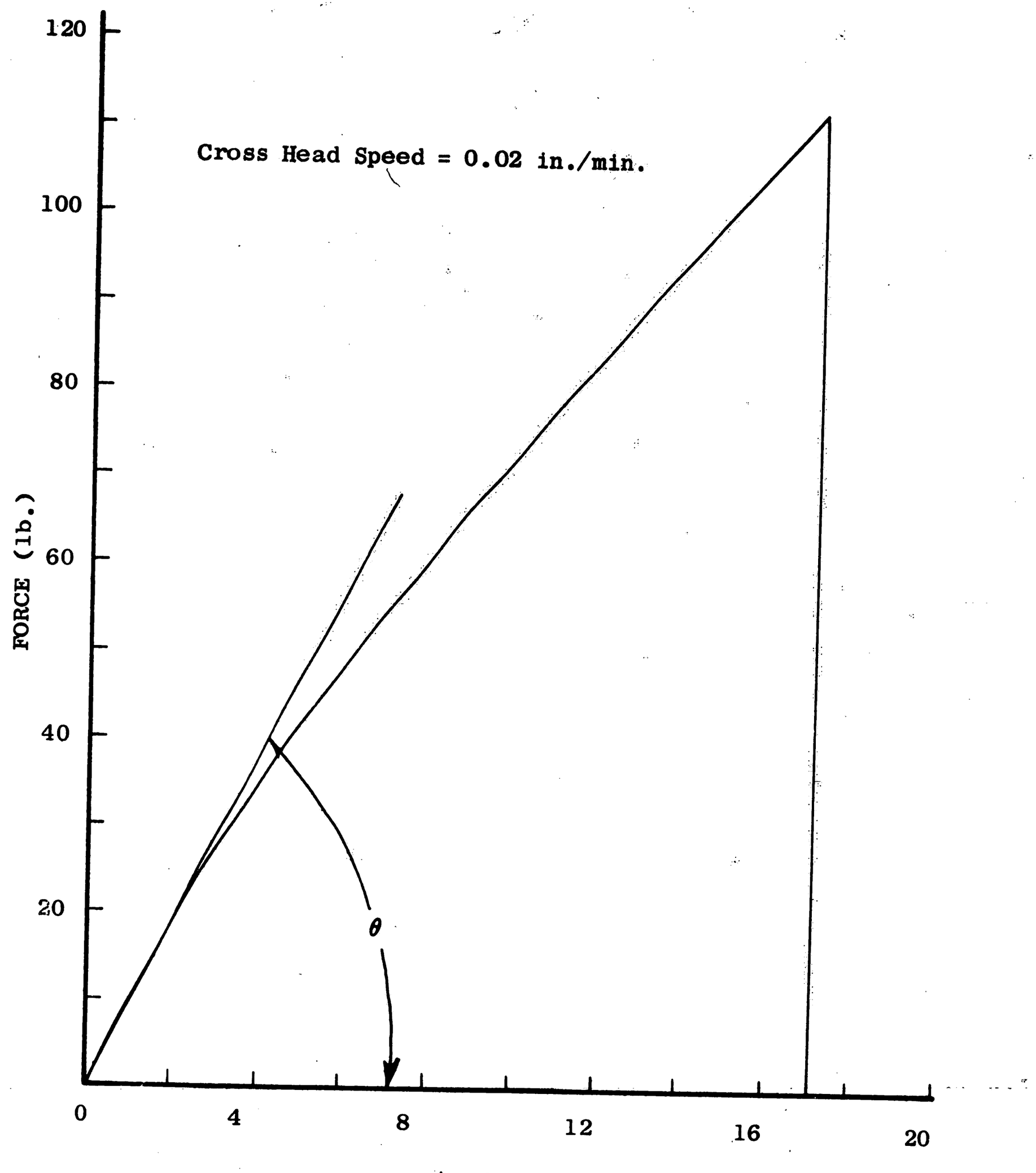

FIGURE 3. TYPICAL TENSILE TEST RESULTS

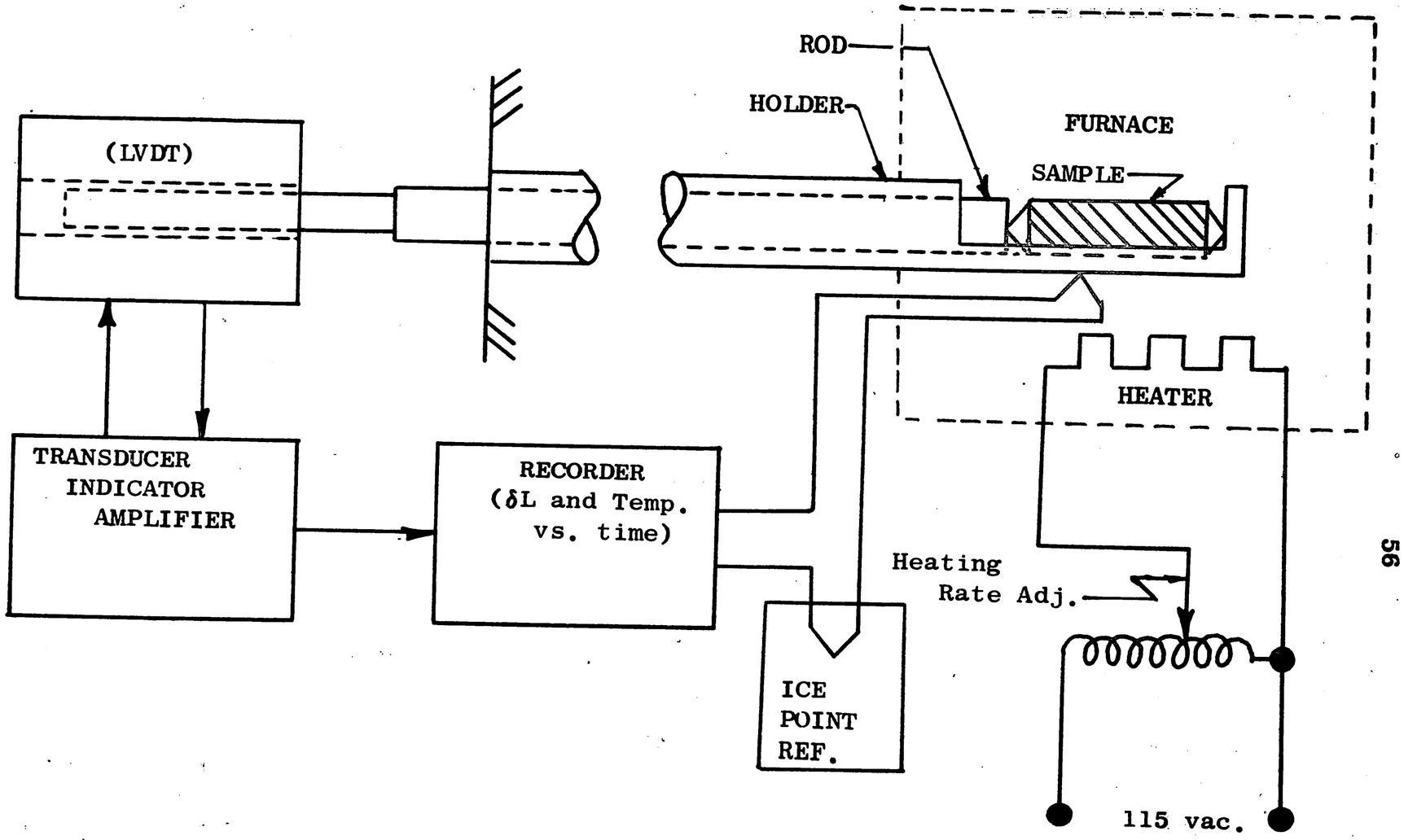

FIGURE 4. BLOCK DIAGRAM OF EXPERIMENTAL SET UP USED IN THERMAL EXPANSION MEASUREMENTS

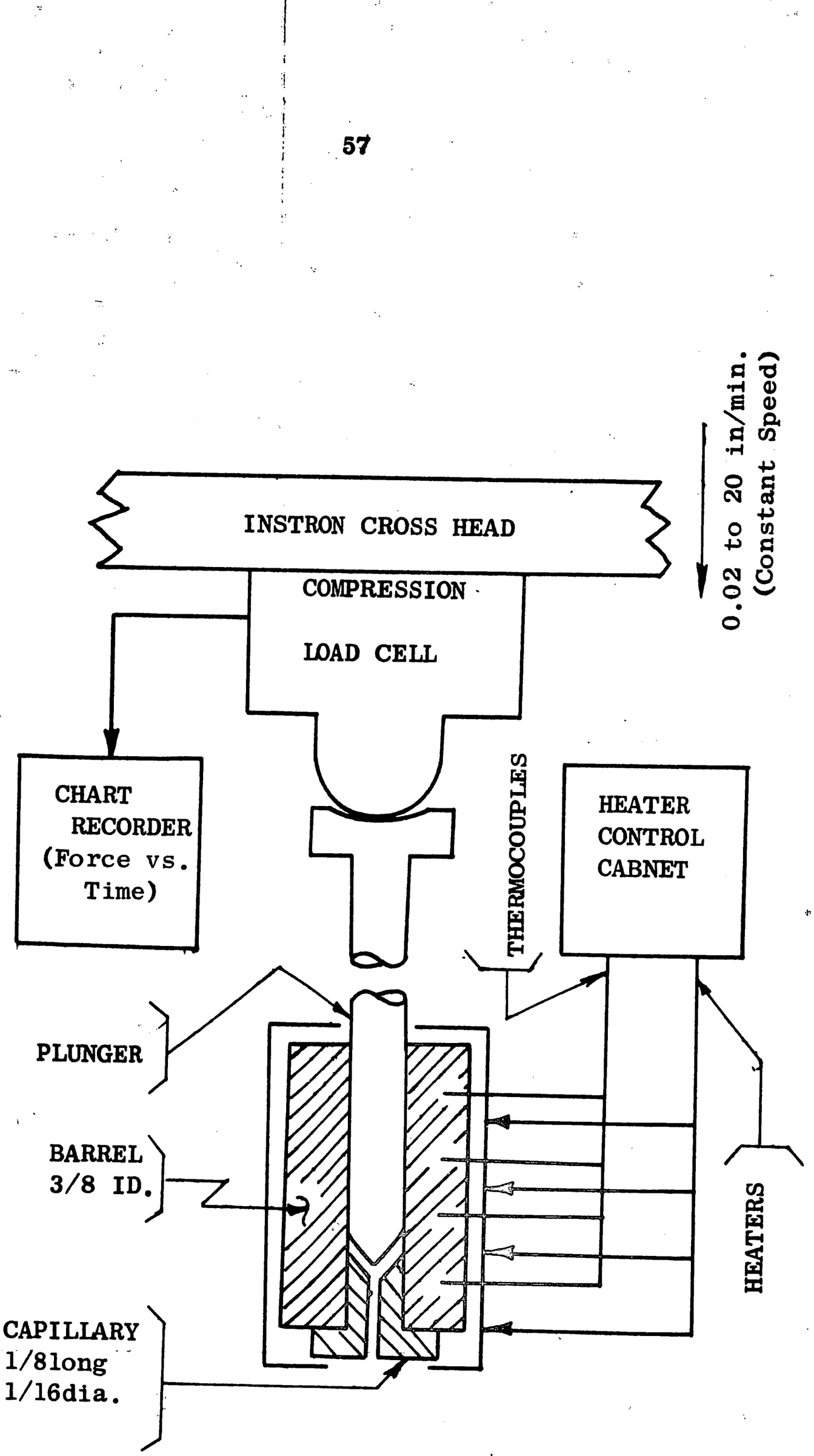

FIGURE 5. SCHEMATIC SHOWING THE ESSENTIAL PARTS OF THE CAPILLARY EXTRUSION RHEOMETER

FIGURE 6· TRANSFER MOLDING PRESS

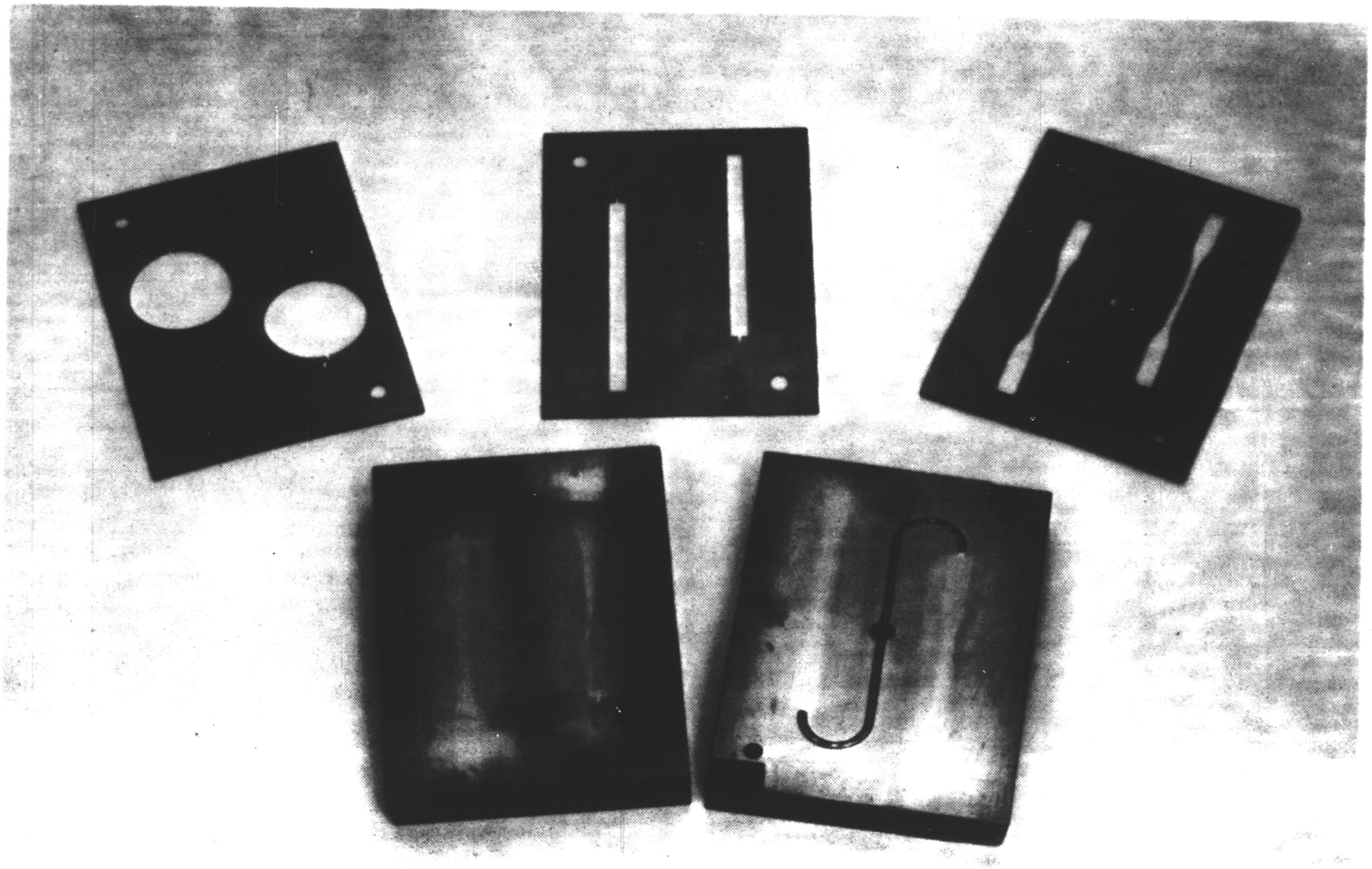

FIGURE 7. MOLD SHOWING INSERTS FOR MOLDING DIELECTRIC, GEHMAN AND TENSILE SAMPLES

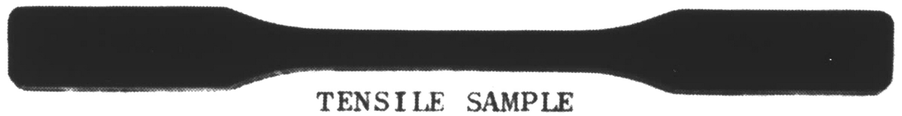

TENSILE SAMPLE

GEHMAN SAMPLE

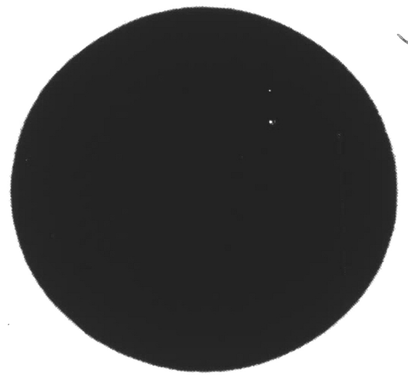

DIELECTRIC SAMPLE

FIGURE 8. TEST SAMPLES

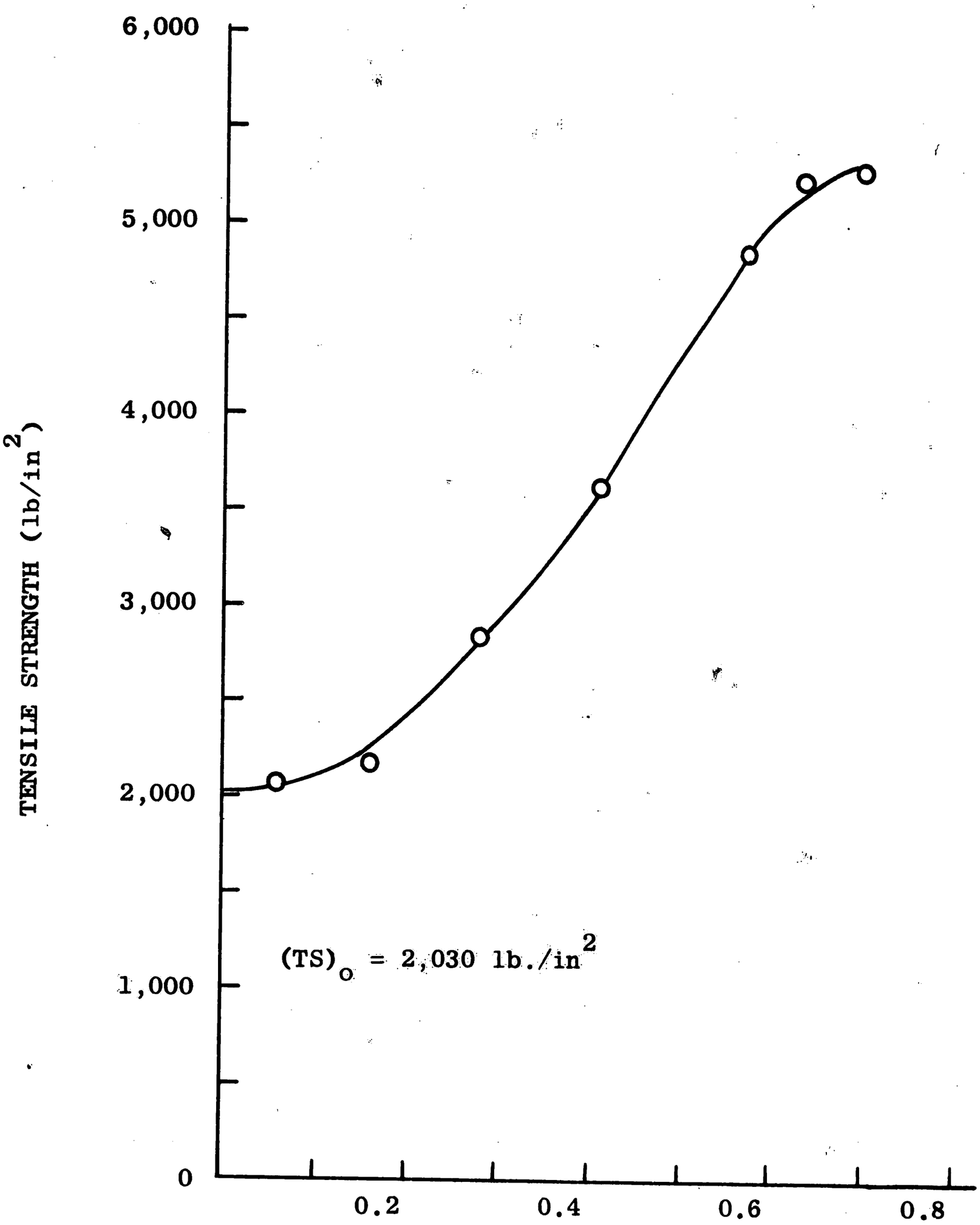

FIGURE 9. TENSILE STRENGTH AS A FUNCTION OF FILLER CONCENTRATION

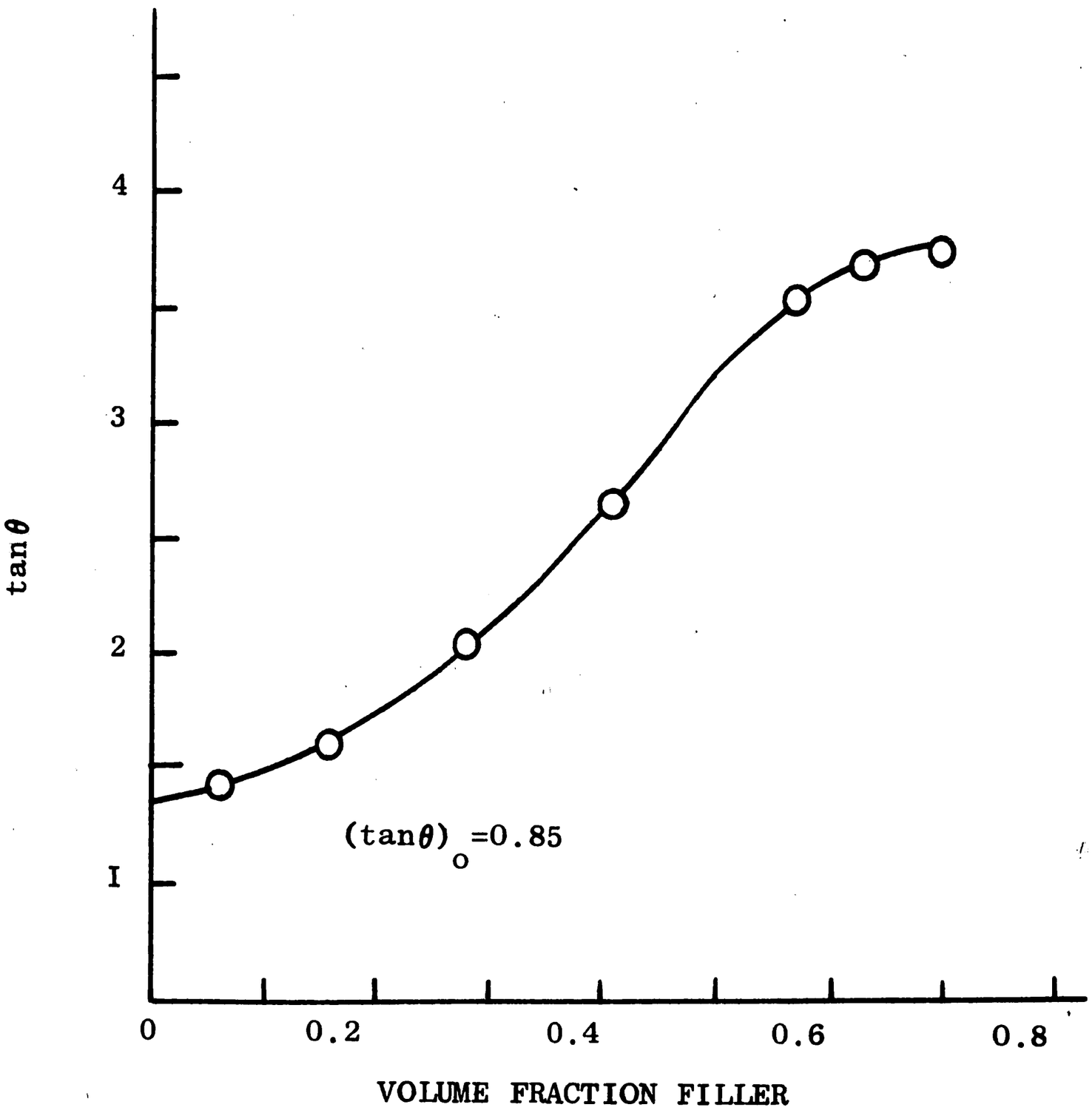

FIGURE 10. INITIAL SLOPE OF TENSILE CURVE AS A FUNCTION OF FILLER CONCENTRATION

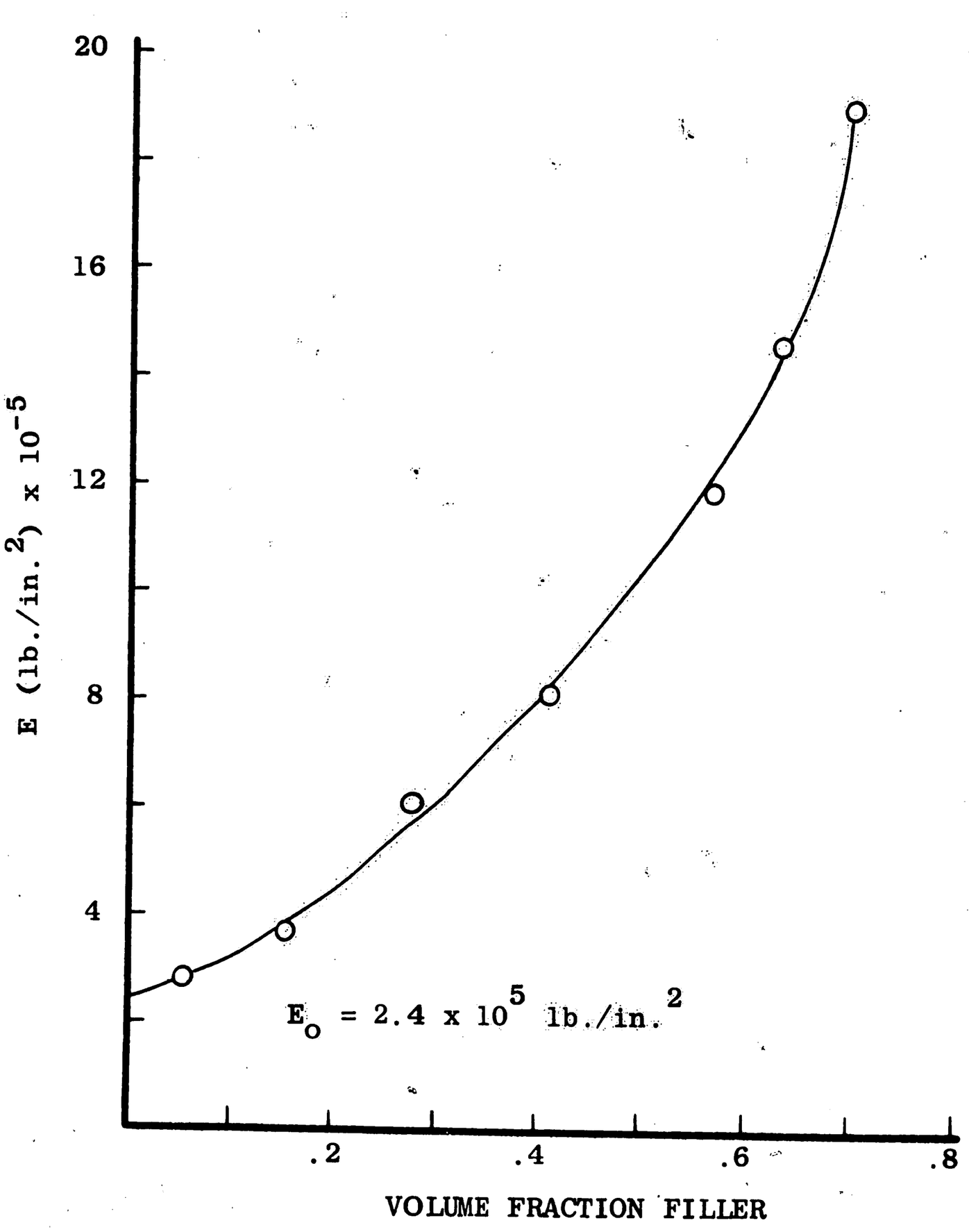

FIGURE 11. MODULUS AS DETERMINED BY MEASUREMENTS WITH GEHMAN FLEX TESTER

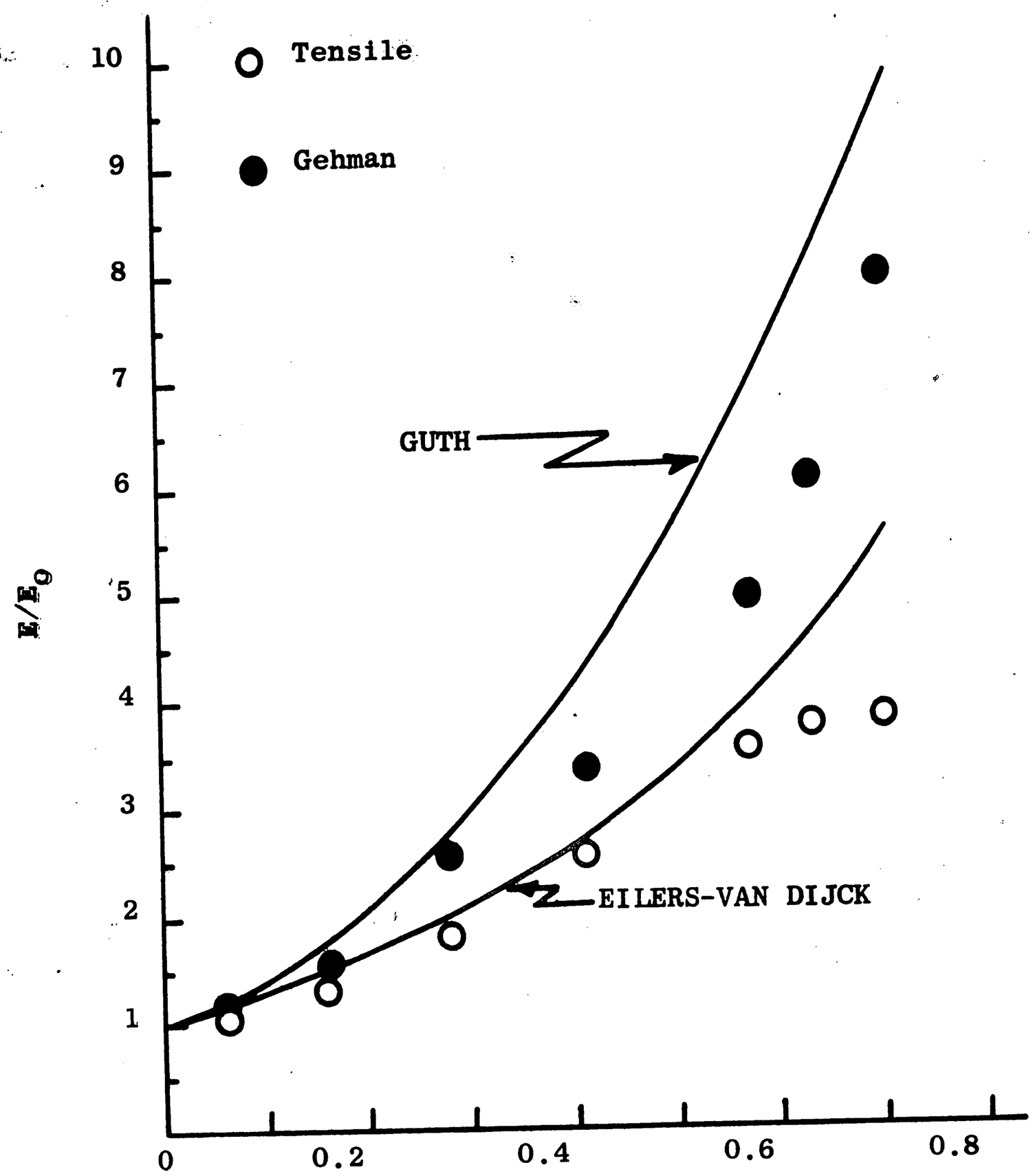

FIGURE 12. RELATIVE MODULUS AS A FUNCTION OF FILLER CONCENTRATION

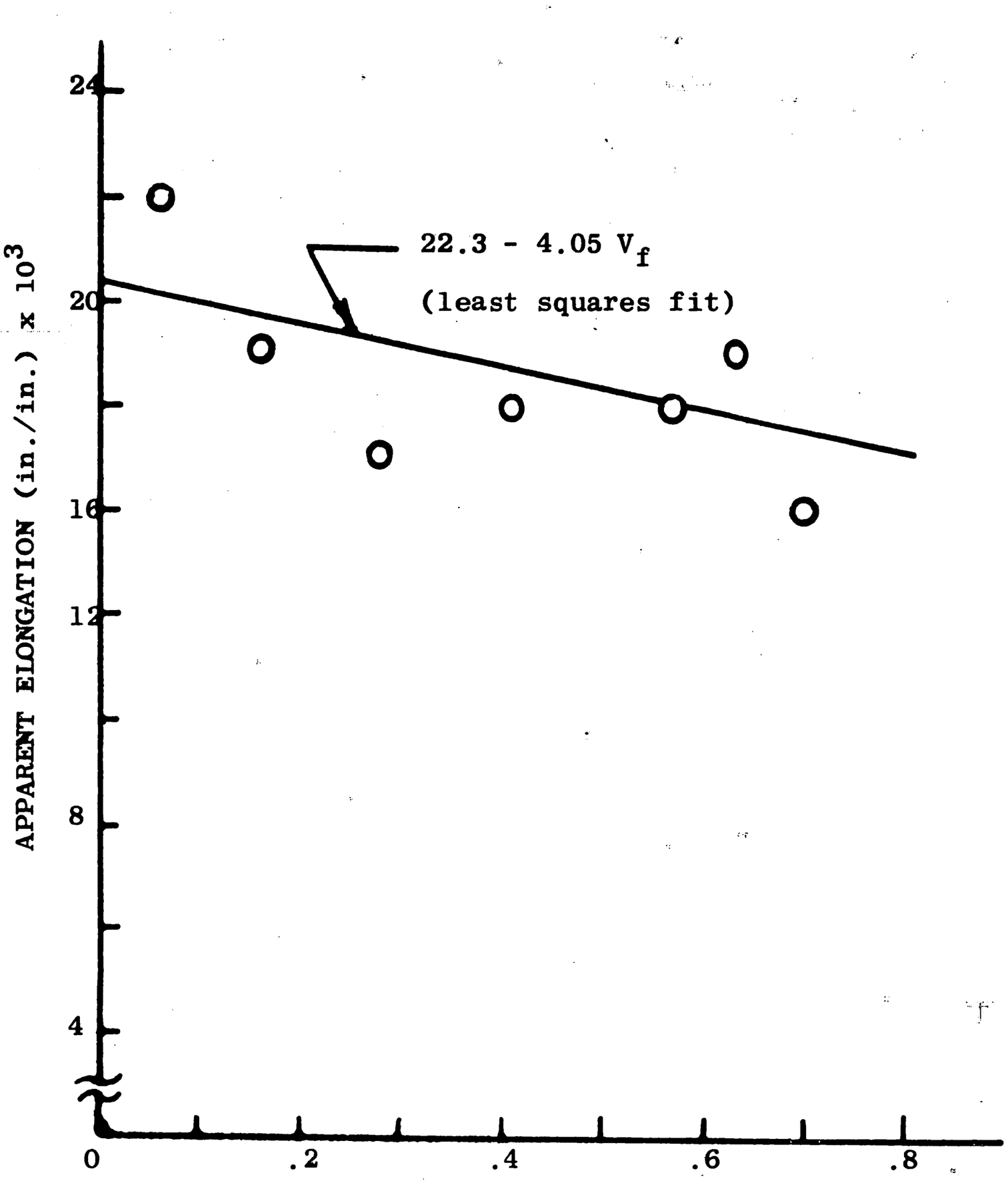

FIGURE 13. APPARENT ULTIMATE ELONGATION AS A FUNCTION OF FILLER CONCENTRATION

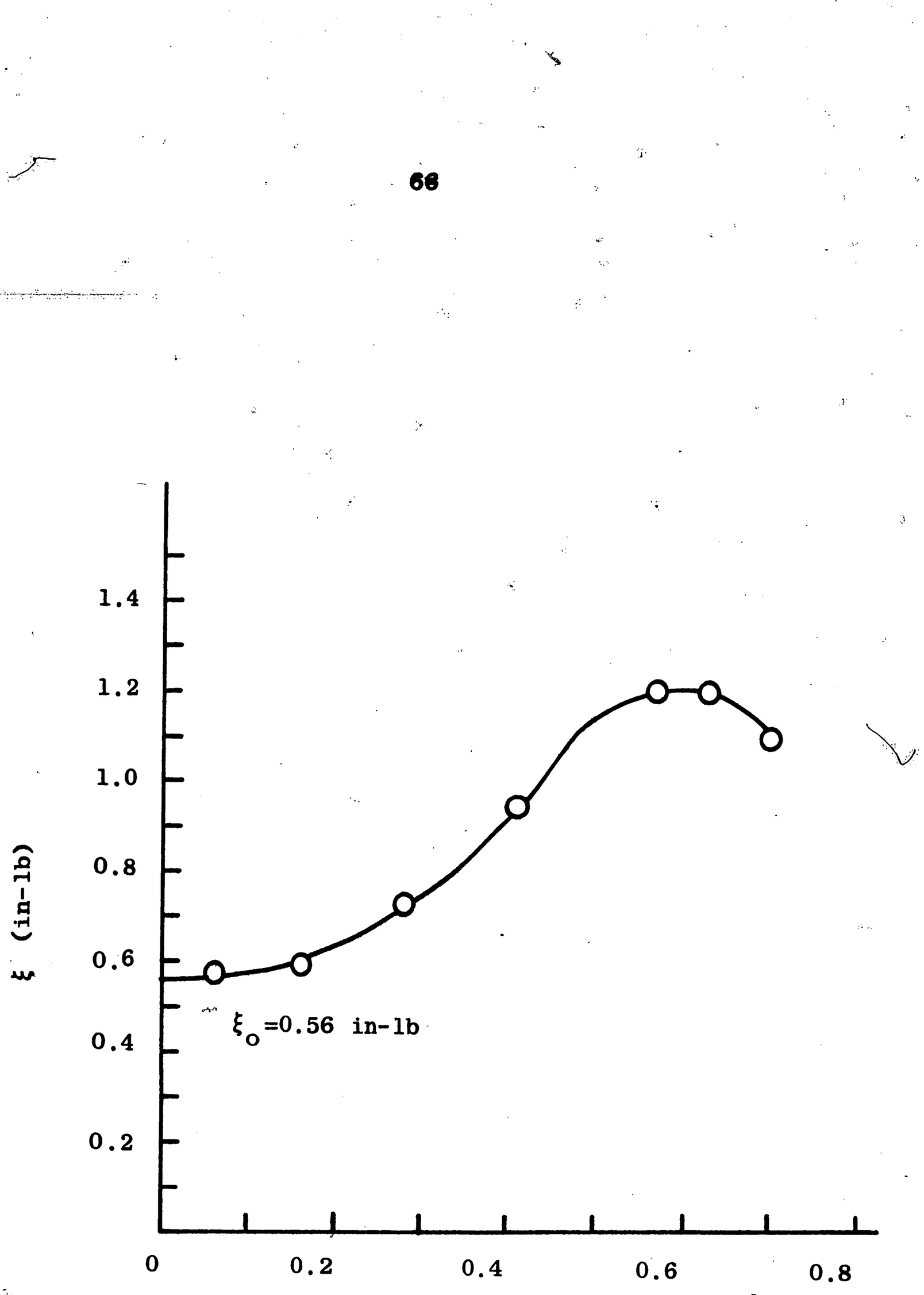

FIGURE 14. FRACTURE ENERGY OF TENSILE SAMPLE AS A FUNCTION OF FILLER CONCENTRATION

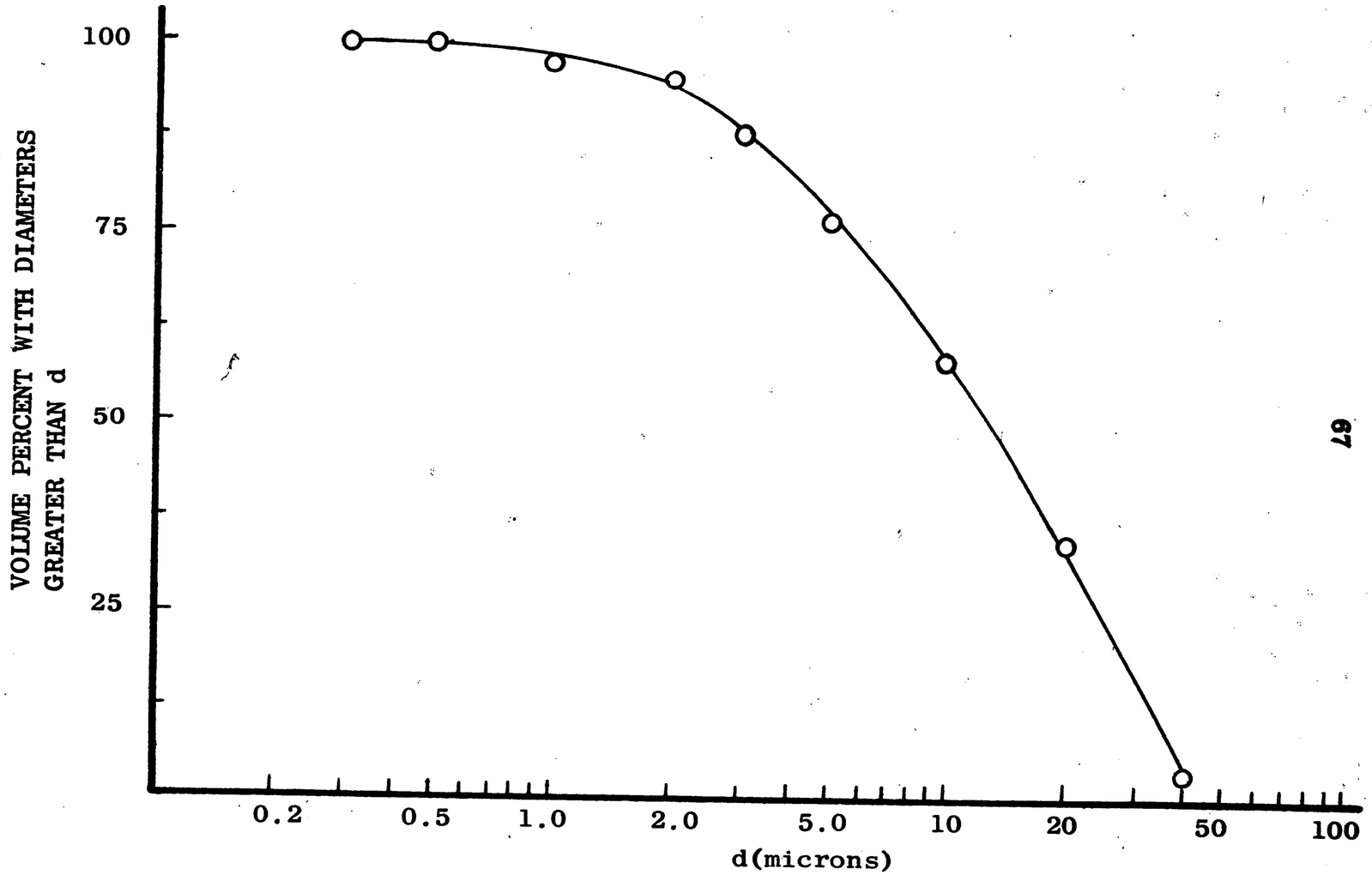

FIGURE 15. PARTICLE SIZE DISTRIBUTION OF STANDARD FILLER USED IN GROUP #1 AND GROUP #2 MATERIALS

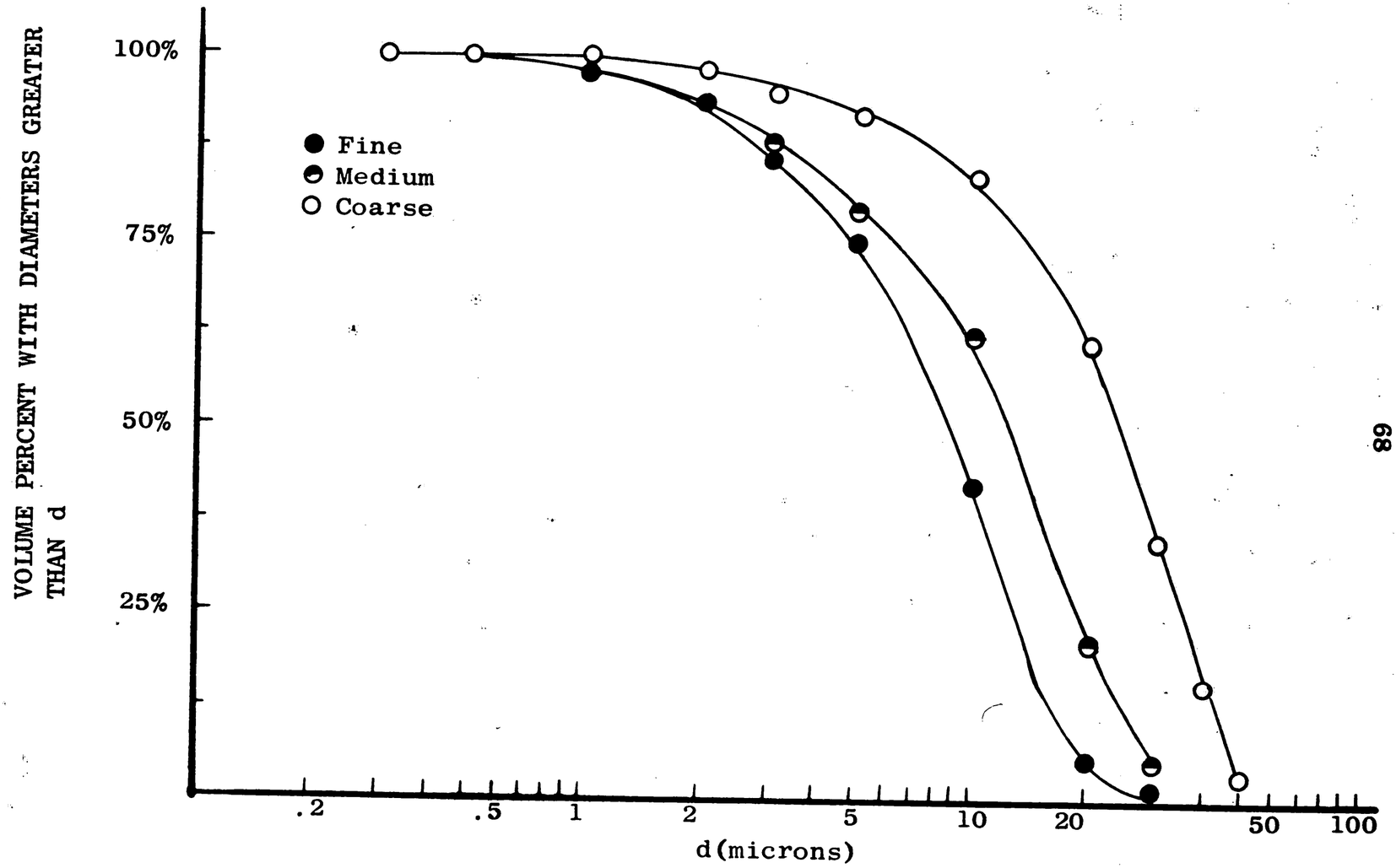

FIGURE 16. PARTICLE SIZE DISTRIBUTION OF ESPECIALLY SEPARATED FILLER USED IN GROUP #3 MATERIAL

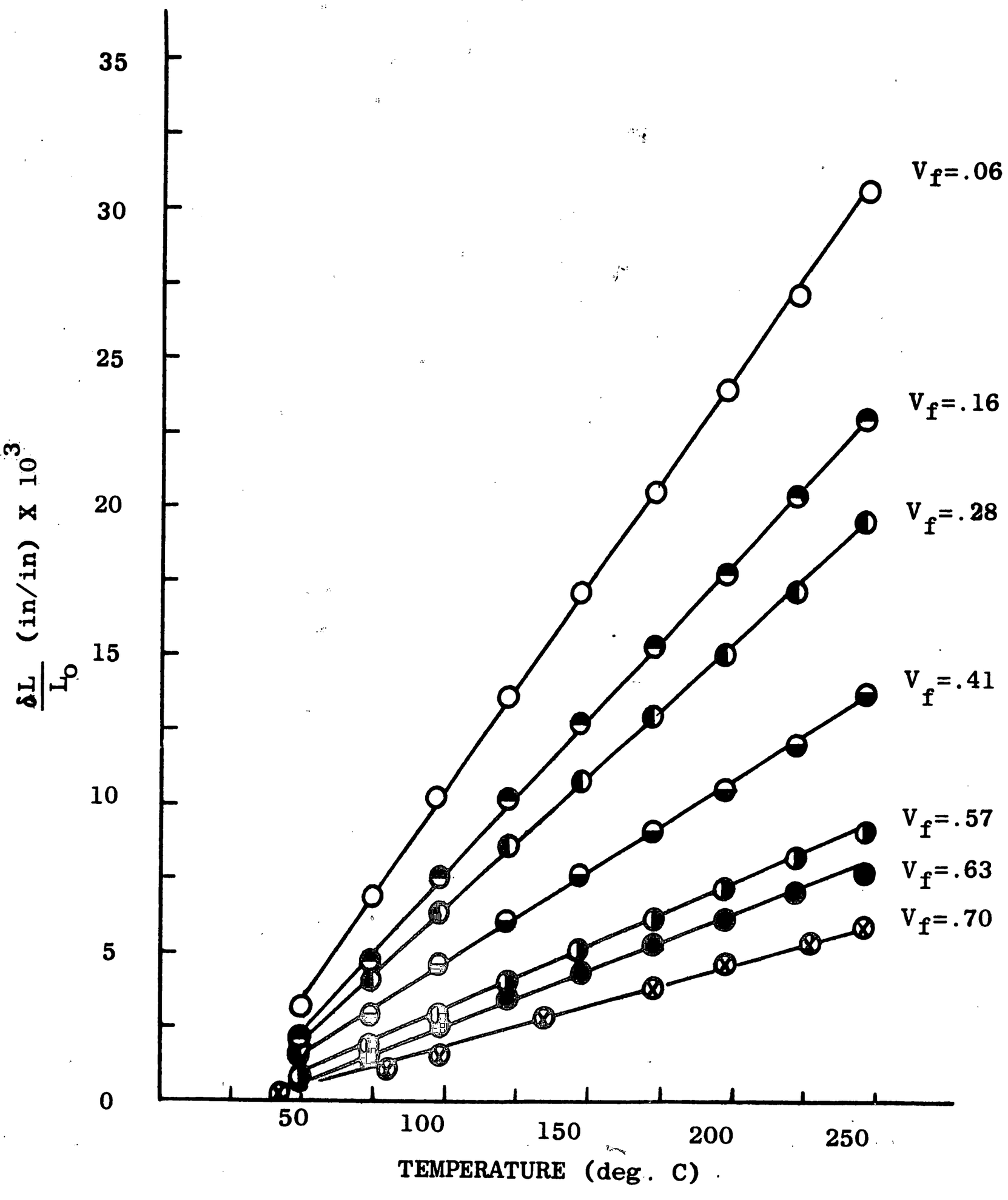

FIGURE 17. THERMAL EXPANSION WITH FILLER CONCENTRATION AS A PARAMETER

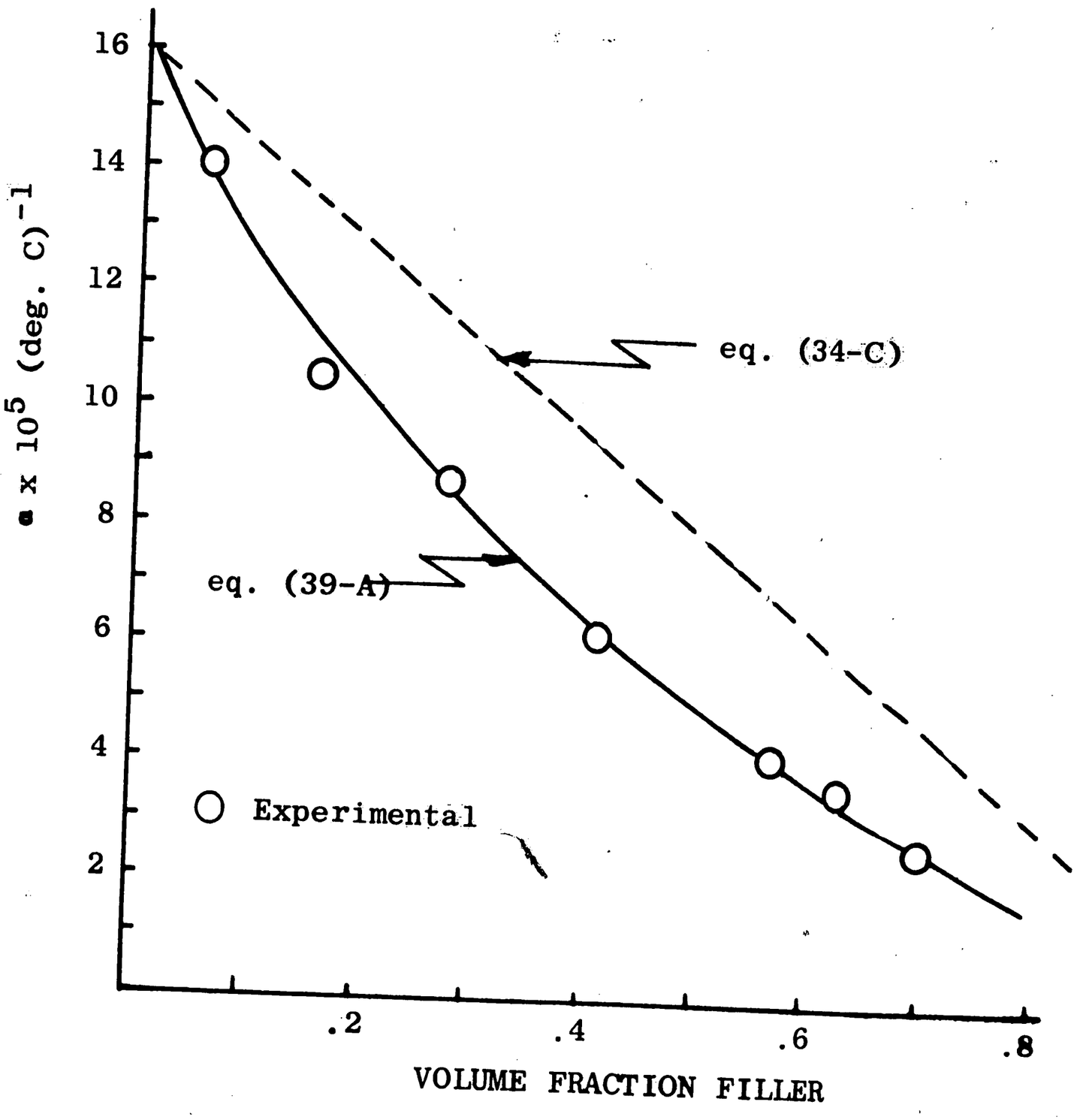

FIGURE 18. COEFFICIENT OF LINEAR THERMAL EXPANSION AS A FUNCTION OF FILLER CONCENTRATION

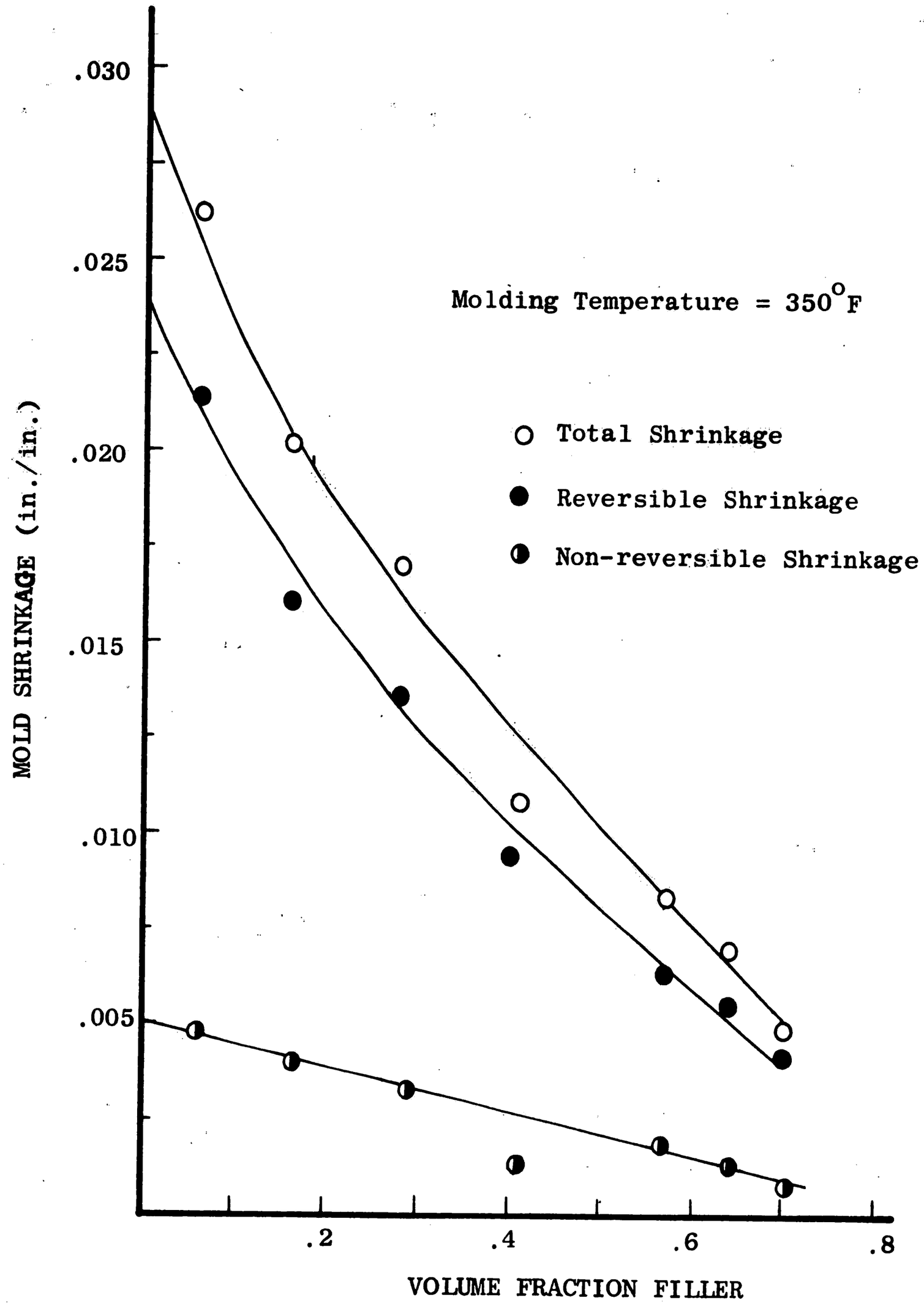

FIGURE 19. MOLD SHRINKAGE AS A FUNCTION OF FILLER CONCENTRATION

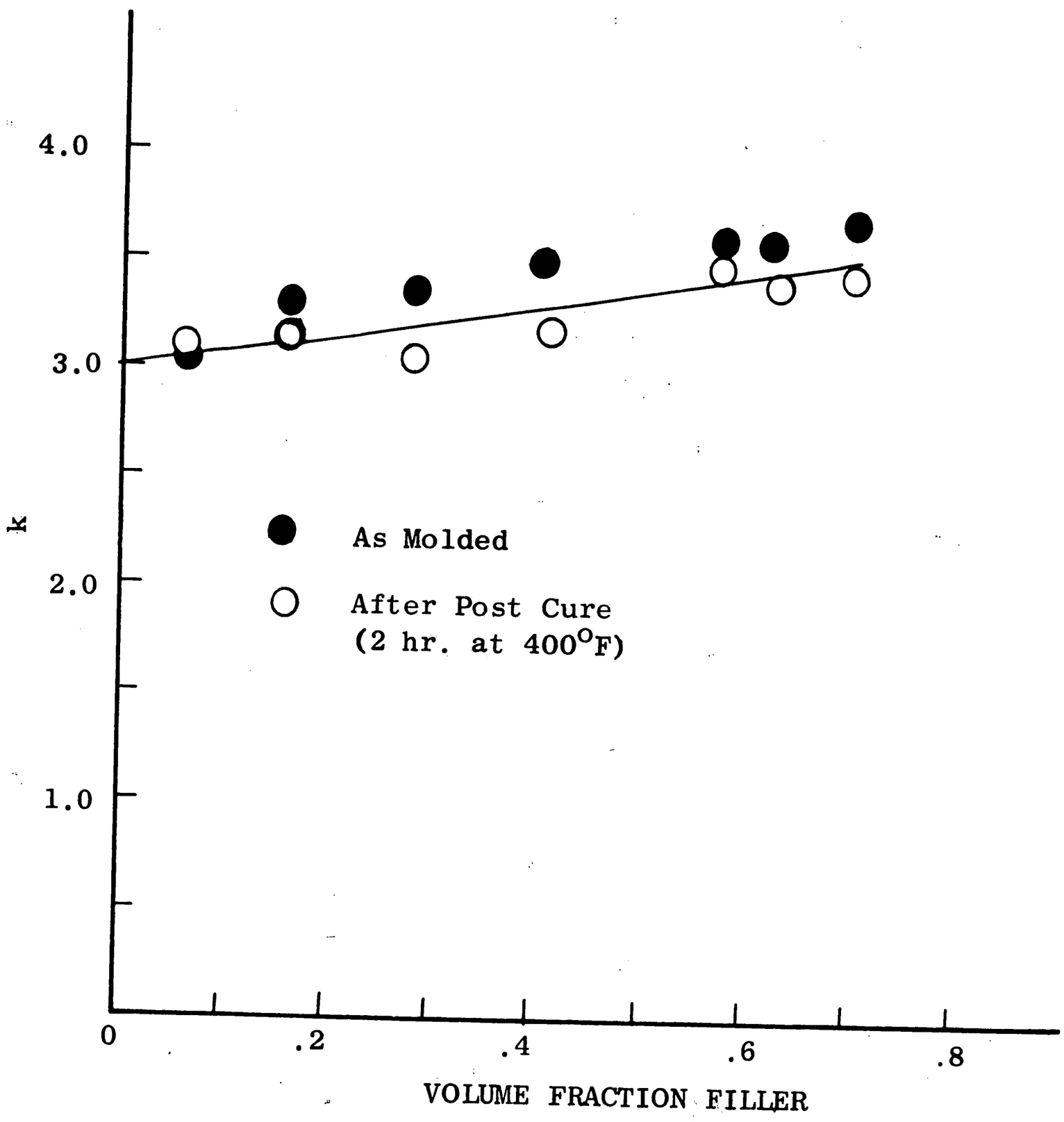

FIGURE 20. DIELECTRIC CONSTANT AS A FUNCTION OF FILLER CONCENTRATION AT 400 Hz.

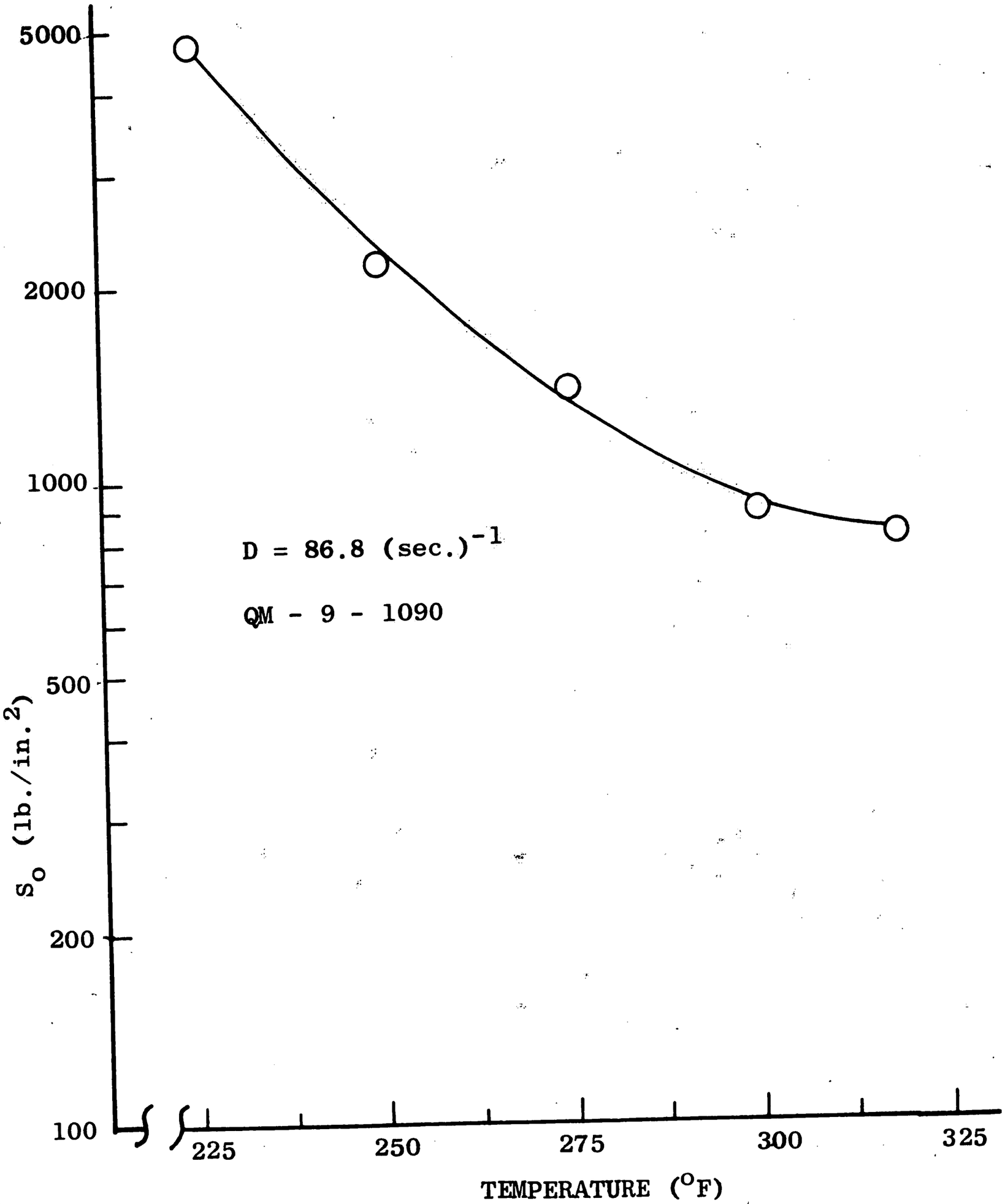

FIGURE 21. MINIMUM SHEAR STRESS AS A FUNCTION OF TEMPERATURE

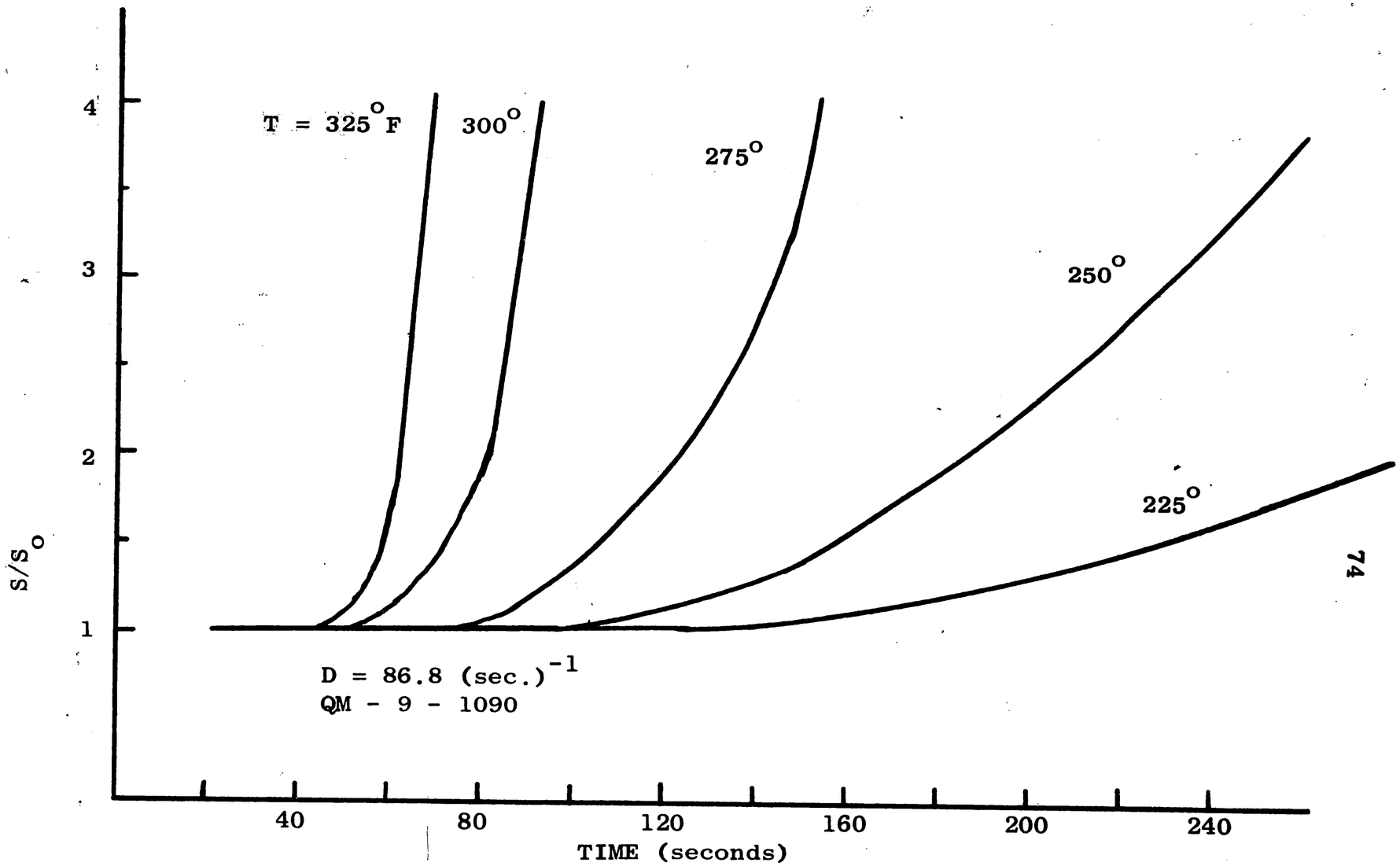

FIGURE 22. NORMALIZED SHEAR STRESS AS A FUNCTION OF TIME WITH TEMPERATURE AS A PARAMETER

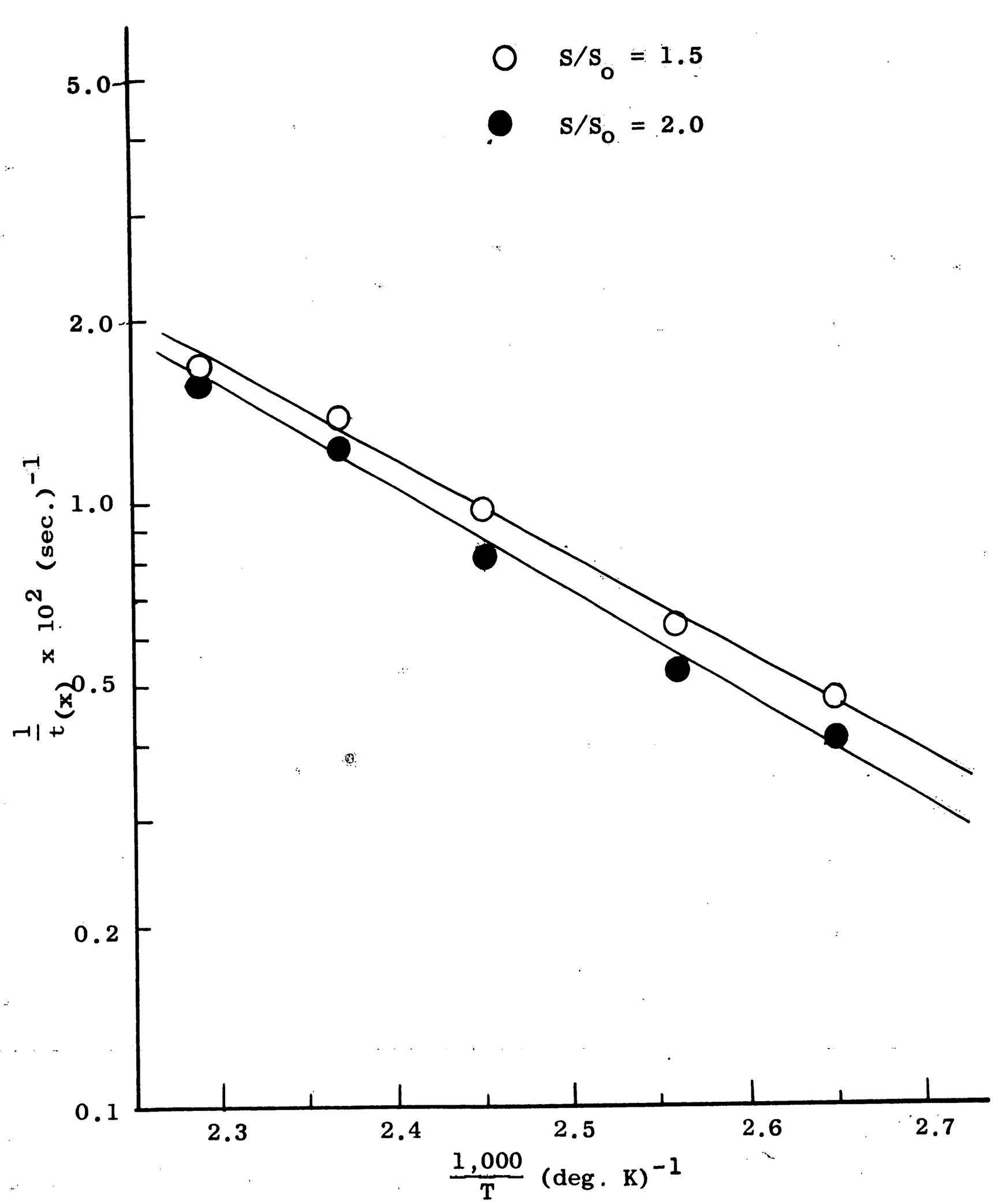

FIGURE 23. HARDENING RATE AS A FUNCTION OF RECIPROCAL ABSOLUTE TEMPERATURE

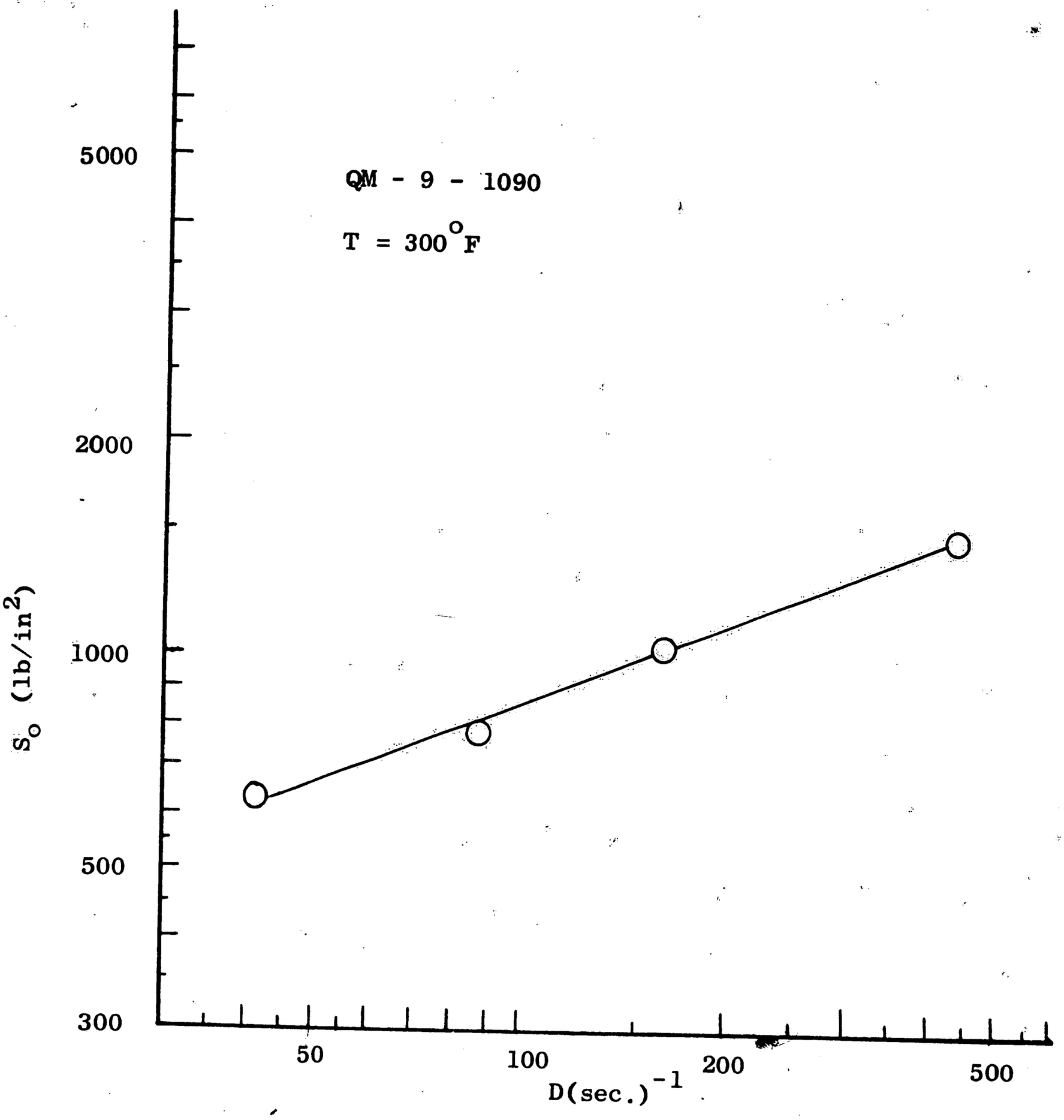

FIGURE 24. MINIMUM SHEAR STRESS AS A FUNCTION OF SHEAR RATE

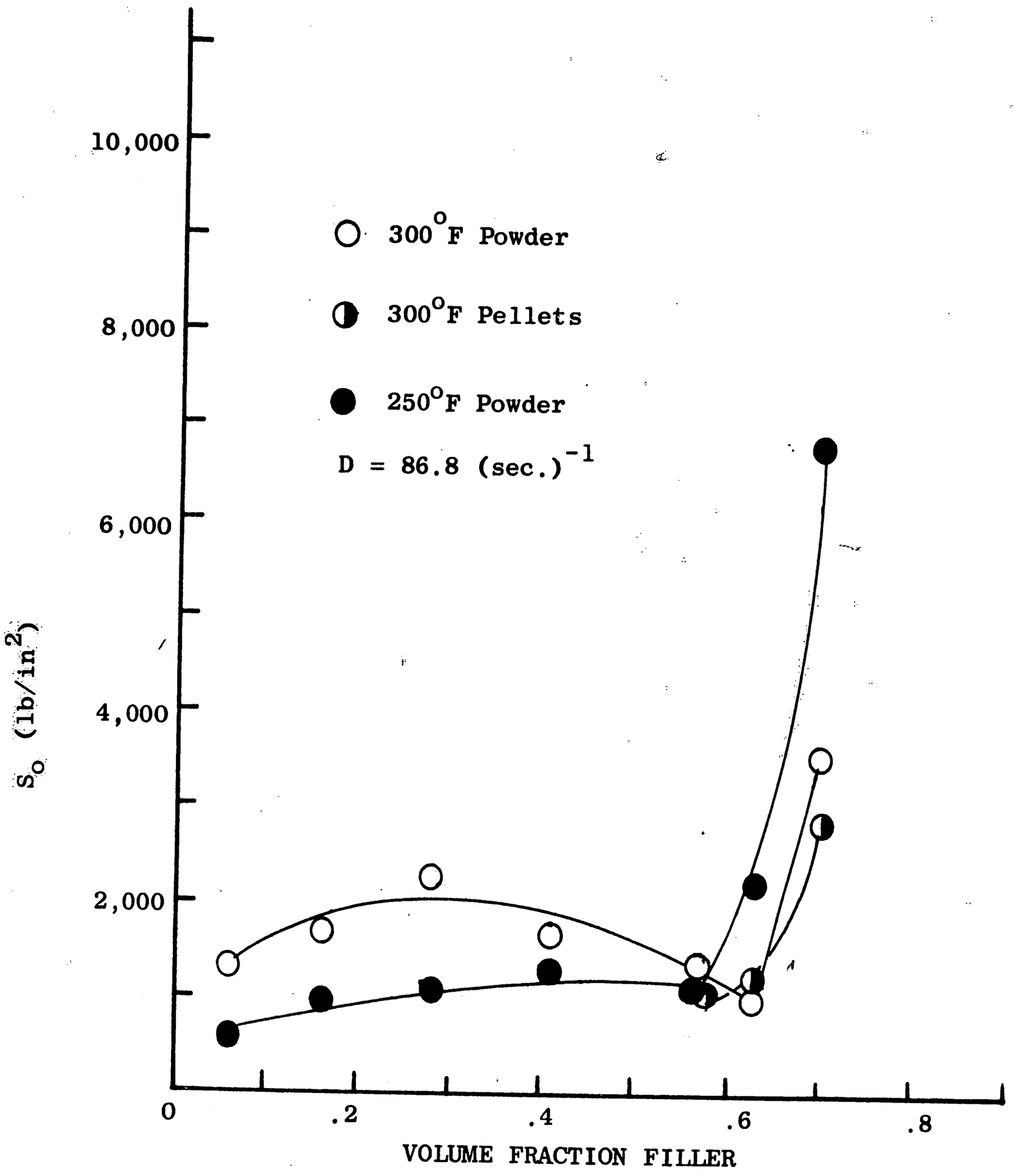

FIGURE 25. MINIMUM SHEAR STRESS AS A FUNCTION OF FILLER CONCENTRATION

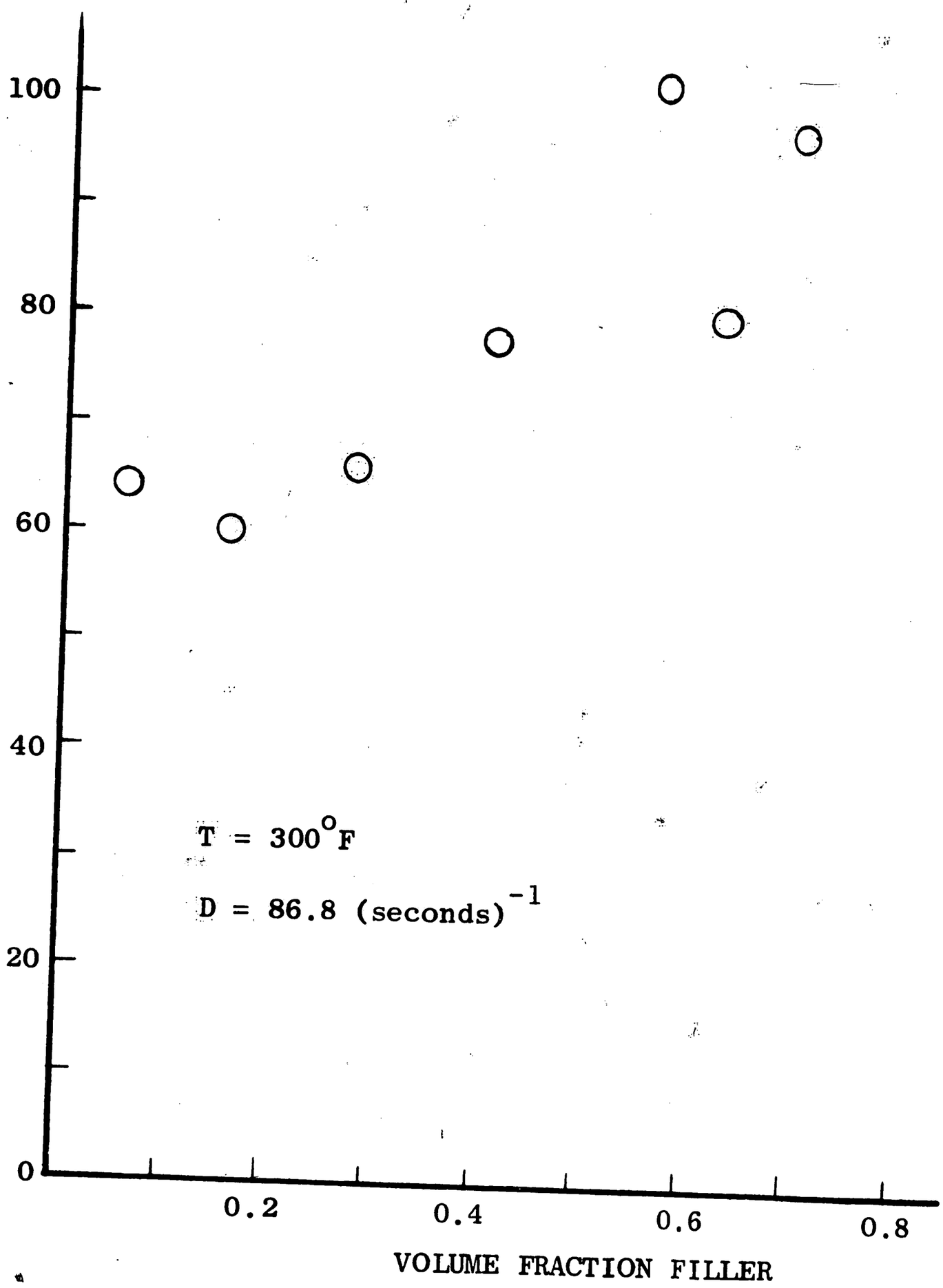

FIGURE 26. THE TIME REQUIRED FOR S/S_o TO REACH A VALUE OF 2 AS A FUNCTION OF FILLER CONCENTRATION

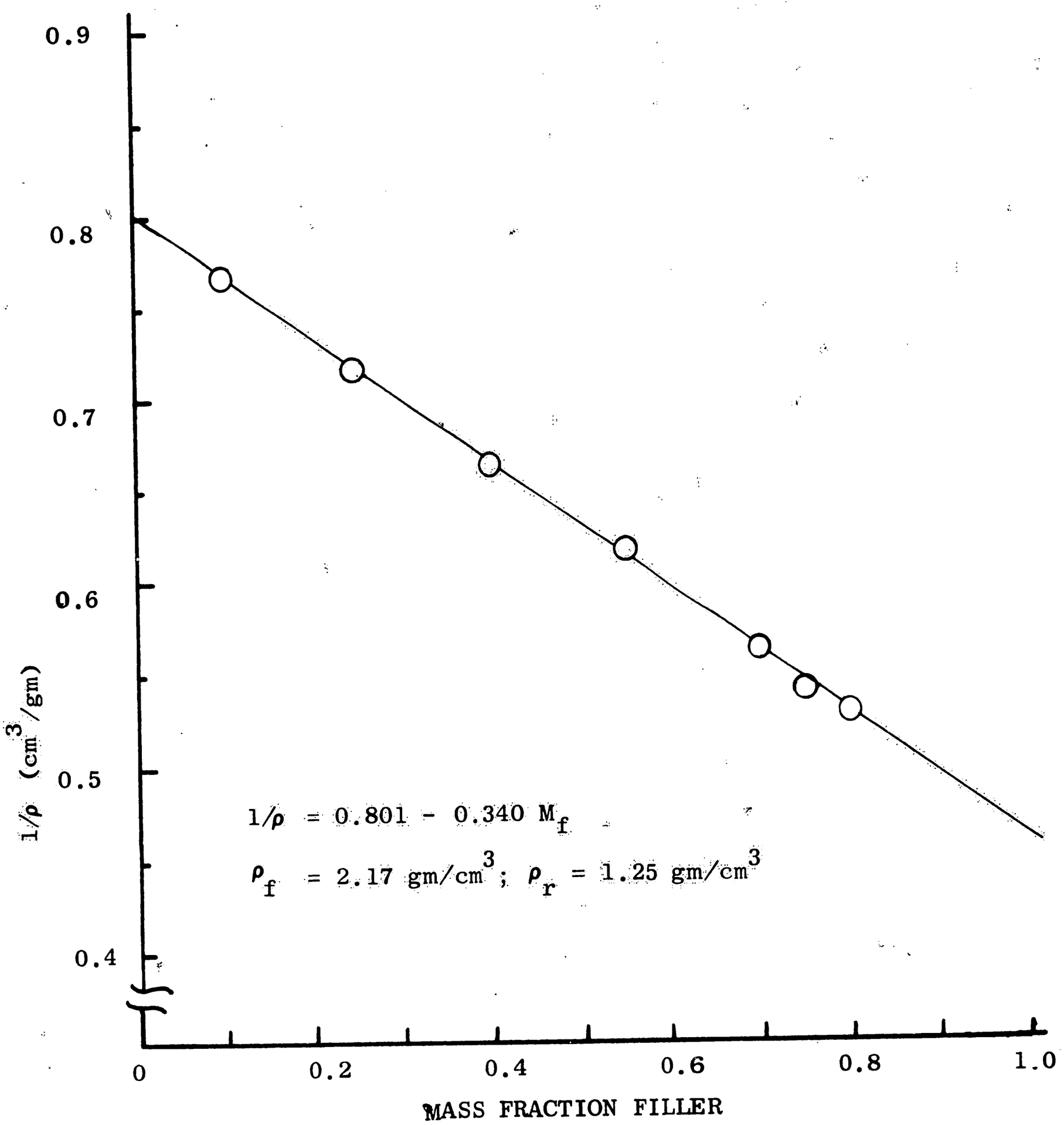

FIGURE 27. RECIPROCAL DENSITY AS A FUNCTION OF FILLER CONCENTRATION

BIBLIOGRAPHY

1 - Meals, R. N., and F. M. Lewis, Silicones, Reinhold Puplishing Corporation, New York, N. Y. (1959).

2 - Guth, E., "Theory of Filler Reinforcement," Journal of Applied Physics, Vol. 16, (1945), p. 20.

3 - Cohan, L. H., "The Mechanism of Reinforcement of Elastomers by Pigments," India Rubber World, Vol. 117, N3, (1947), p. 343.

4 - Bueche, A.\M., "Filler Reinforcement of Silicone Rubber," Journal of Polymer Science, Vol. 25, (1947), p. 139.

5 - Blanchard, A. F., and D. Parkinson, "Breakage of Carbon-Rubber Networks by Applied Stress," Industrial and Engineering Chemistry, Vol. 44, N-4, (1952), p. 799.

6 - Bueche, F., Physical Properties of Polymers, Interscience Pub., New York, New York, (1962).

7 - Sato, Yoshiyasu and Junji Furukaua, "A Molecular Theory of Filler Reinforcement Based on the Concept of Internal Deformation," Rubber Chemistry and Technology, Vol. 36, (1963), p. 1081.

8 - Nielsen, L. E., "Simple Theory of Stress-Strain Properties of Filled Polymers," Journal of Applied Polymer Science, Vol. 10, (1966), p. 97.

9 - Rehner, J., Jr., "Thermodynamics and Mechanics of Filler Reinforcement," Journal of Polymer Science, Vol. 7, (1951), p. 519.

10 - Alter, H., "Filler Particle Size and Mechanical Properties of Polymers," Journal of Applied Polymer Science, Vol. 9, (1965), p. 1525.

11 - Warrick, E. L. and P. C. Lauterbur, "Filler Phenomena in Silicone Rubber," Industrial and Engineering Chemistry, Vol. 47, (1955), p. 486.

12 - Varadhachary, S. N., "Finger Printing Thermoset Molding Compounds Through Dynamic Flow Testing," Society of Plastic Engineers Journal, Vol. 23, N-6, (1967).

BIBLIOGRAPHY (cont.)

13.- Salyer, I. O., J. W. Heyd, R. M. Brodbeck, L. W. Hartyel, and L. E. Brown, "Use of Capillary Extrusion Rheometer to Measure Curing of Thermosetting Plastics and Rubbers," Journal of Polymer Science, (Part A), Vol. 3, (1965), p. 1911.

14.- Smith, T. L., "Measurement and Analysis of Small Deformation and Ultimate Tensile Properties of Amphorous Polymer," Application Series, PC-5, Instron Engineering Corp., Canton, Mass.

15.- Tobolsky, A. V., Properties and Structure of Polymers, John Wiley and Sons, New York (1960).

16 - Standard Method of Test for the Coefficient of Linear Thermal Expansion of Plastics. ASTM - D696-44 Adopted 1944 and in 1961 without change.

17 - Gray, D. E. (Coordinating Editor) American Institute of Physics Handbook, McGraw-Hill, New York, (1957).

18 - Instruction Manual for Type 1690A Dielectric Sample Holder, General Radio Company, West Concord, Mass.

19 - Tentative Method of Test for A-C Capacitance, Dielectric Constant, and Loss Characteristic of Electrical Insulating Materials, ASTM - 150 - 59T, American Society for Testing Materials, Philadelphia, Penna., (1959)

20 - Merz, E. H. and R. E. Colwell, "A High Shear Rate Capillary Rheometer for Polymer Melts," ASTM Bullitin No. 232, Sept. 1958, American Society for Testing Materials, Philadelphia, Penna.

21 - Manufacturer's information - Miller Air Cylinder.

22 - Tentative Method of Test for Tensile Properties of Plastics ASTM D - 638 - 61T, American Society for Testing Materials, Philadelphia, Penna., (1961)

23 - Karnowsky, M. M. and J. L. Colp, "A Small Tensile Test Specimen for Plastics," Materials, Research and Standards, Vol. 4, p-351-4 (1964).

24 - Information About Electronic Materials, Dow Corning Bullitin: 07 - 239, Dow Corning Company, Midland, Mich., January 1967.

BIBLIOGRAPHY (cont.)

25 - Gilbride, E. and S. B. Levinson, "Limestone Fillers in Epoxy Systems" Modern Plastics, Vol. 42, N-11, (1965), pp. 147 - 149.

26 - J. H. Bachman, J. W. Sellers, M. P. Wagner and R. F. Wolf, "Fine Particle Reinforcing Silicas and Silicates In Elastomers," Rubber Chemistry and Technology, Vol. 32, (1959), pp. 1286 - 1391.

27 - Van Der Wal, C. W., H. W. Bree, and Schwarzl "Mechanical Properties of Highly Filled Elastomers. II. Relationship Between Filler Characteristics, Thermal Expansion, and Bulk Moduli," Journal of Applied Polymer Science, Vol. 9, (1965) pp. 2143 - 2166.

28 - Darken, L. S. and R. W. Gurry, Physical Chemistry of Metals, McGraw-Hill, New York, (1953), p. 181.

29 - Looyenga, H., "Dielectric Constants of Hetrogeneous Mixtures," Physica, Vol. 31, (1965), pp. 401 - 406.

30 - Kingery, W. D., Introduction to Ceramics, John Wiley and Sons, New York, (1960), p. 706.

31 - Hand Book of Physics and Chemistry, 34th edition, Chemical Rubber Publishing Company, Cleveland, Ohio (1952).

32 - M-S-A Particle Analyzer - Operating Proceedures and Applications, Mine Safety Appliances Company, Pittsburg, Penna.

VITA

Robert O. Bridges was born October 21, 1933 in Forest City, North Carolina, the son of James W. Bridges (deceased) and Annie Owen Bridges (deceased).

Mr. Bridges graduated from Mount Vernon High School, Forest City, North Carolina, in 1952. Beginning in January 1953 he served a four year enlistment in the U. S. Air Force where he was a radio repairman. After being honorably discharged in December 1956, he entered North Carolina State University where he received the degree of Bachelor of Science in Electrical Engineering in June 1961.

Since graduation, Mr. Bridges has been employed by the Western Electric Company. From June 1961 to September 1964 he was an engineer assigned to a power supply development group in Winston-Salem, North Carolina; from September 1964 until June 1966 he worked as a Test Planning Engineer at Allentown, Pennsylvania. Since June 1966 he has been a Lehigh Master's candidate at the Western Electric Engineering Research Center in Princeton, New Jersey.

Mr. Bridges is a member of Eta Kappa Nu.